People's Democratic Rebuplic of Algeria
Ministry of Higher Education and Scientific Research

University of Shahid Hamma LakhderEL-OUED
Faculty of Natural and Life Sciences
Department of Cellular and Molecular Biology

MASTER'S THESIS

For the obtention of the Academic Master's Degree in Biological Sciences

Specialization: **Toxicology**

TITLE

Formulation of a sunscreen based on zinc oxide nanoparticles and (*Daucus carrot.L*) seeds

Presented by:

Nihed Yasmine BELAID Rahma MASSAOUDI

Before the jury composed of

Dr. Lanez ELhafnaoui **Committee Chair**

Dr. Tedjani Aicha **Examiner**

Dr. Chenna djehad **Incubator Representative**

Dr. Adel Gharbi **Incubator Representative**

Dr. Said TOUATI **Supervisor**

Dr. Chaima BENINE **Co-supervisor**

Academic year: 2025/2026

ACKNOWLEDGEMENTS

In the first place, we stand in humble gratitude before Almighty Allah for bestowing upon us the patience, diligence, and determination required to undertake this academic endeavor and fulfill our aspirations.

We would like to articulate our deepest appreciation to our supervisor, **Dr. Touati Said,** for his valuable guidance, continuous support, and constructive advice throughout the realization of this work. His supervision and encouragement have been instrumental in completing this dissertation.

We would also like to express our sincere gratitude to Mrs. **Benine Chaima**, co-supervisor of this study, for her assistance, support, and valuable recommendations. Her contributions and availability were greatly appreciated throughout the different stages of this research.

We are highly honored and deeply privileged that jury members have graciously accepted to evaluate this dissertation. We extend to them our highest consideration, utmost respect, and sincere gratitude for their time and dedication in serving on the examination committee and enriching this work with their expertise.

Finally, we owe a debt of gratitude to our colleagues, friends, and everyone who, through their encouragement, kindness, or assistance whether directly or indirectly contributed to the realization of this endeavor.

اهــــداء

الحمد لله أو الً وآخ ارا، الذي بنعمته تتم الصالحات، وبتوفيقه تُنجز الأعمال، وله الشكر على ما منح ويسّر وأعان.

إلى أبي وأمي، بكل الحب والمَتنان، أستمد من حضورهما القوة، ومن دعائهما السند والأمان، فلهما الفضل بعد الله في كل خطوة وصلتُ إليها.

إلى إخوتي وأخواتي، أحبّكم من القلب، وأنتم الدفء الذي أجد فيه السند والطمأنينة، ووجودكم يمنح حياتي معنى أجمل وراحة لً تُوصف.

إلى أختي الصغرى سجاء، التي تملأ أيامي بدعمها وابتسامتها، وتمنح لحياتي بهجة خاصة لً تشبه أح ادا.

إلى نفسي...

إلى تلك التي كافحت بصمت، وواصلت الطريق رغم التعب، وكانت سندا لنفسها حين احتاجت القوة، ونهضت في كل مرة حتى بلغت هذه المرحلة. أكتب لها اليوم بكل فخر؛ لأنها لم تستسلم، ولأنها اختارت الاسَتمرار رغم كل شيء.

إلى كل من ساهم من قريب أو بعيد في تشجيعي على طلب العلم ومواصلة الاجتهاد، وإلى كل من فرح لنجاحي وتمنى لي الخير.

وختاما...

في الصبر مشقته، لكن يعقبه فرج جميل، وما هذا الإنجاز إلً ثمرة صبرٍ طويل ويقين بأن الله لن يضيع أجر من أحسن عملا.

بالعيد نهاد ياسمين

بسم الله الرحمن الرحيم

﴿وَقُلْ رَبِّ زِدْنِي عِلْمًا﴾

الحمد لله الذي وفقني وأعانني على إتمام هذا العمل، ووهبني القوة والصبر لأصل إلى هذه المرحلة المهمة من حياتي.

أهدي ثمرة جهدي وتخرجي إلى أغلى الناس على قلبي، إلى والديّ العزيزين، اللذين كانا النور الذي أنار دربي، والسند الذي استندت إليه في كل خطوة من خطوات حياتي. إليهما أهدي هذا النجاح تقديرًا لما قدماه لي من حب ورعاية وتضحيات لا تُقدَّر بثمن، راجية من الله أن يحفظهما ويجزيهما عني خير الجزاء.

إلى إخوتي وأخواتي، الذين كانوا مصدرًا للفرح والقوة والدعم، وشاركوا معي لحظات التعب والأمل، فكانوا خير معين لي في هذه المسيرة.

إلى عائلتي الكبيرة، التي كانت دائمًا إلى جانبي بالدعاء والتشجيع والكلمات الطيبة التي منحتني الثقة والعزيمة لمواصلة الطريق.

إلى صديقاتي وزميلاتي، اللواتي تقاسمن معي سنوات الدراسة بما حملته من تحديات وذكريات جميلة ستبقى محفورة في الذاكرة، شكرًا لكل لحظة دعم ومساندة ورفقة صادقة.

إلى كل من ساهم من قريب أو بعيد في تشجيعي على طلب العلم ومواصلة الاجتهاد، وإلى كل من فرح لنجاحي وتمنى لي الخير.

وأخيرًا، أهدي هذا العمل إلى نفسي، التي واجهت الصعوبات وتجاوزت العقبات، وتحملت ضغوط الدراسة والبحث حتى وصلت إلى هذه اللحظة، لحظة جني ثمار سنوات من الجد والاجتهاد.

أسأل الله أن يجعل هذا العمل خالصًا لوجهه الكريم، وأن ينفع به، وأن يكون بداية لمستقبل مليء بالنجاح والعطاء.

مسعودي رحمة.

Formulation of a sunscreen based on zinc oxide nanoparticles and (*Daucus carrot.* L)

Abstract

The growing demand for natural and effective ultraviolet (UV) protective formulations has increased interest in the green synthesis of plant-based nanoparticles for cosmetic applications. This study aimed to synthesize zinc oxide nanoparticles (ZnO-NPs) through a green approach using the aqueous extract of *Daucus carota L.* seeds as both a reducing and stabilizing agent, and to evaluate their biological properties and UV-protective potential. Phytochemical analysis revealed a high content of phenolic compounds, followed by tannins and flavonoids, with an extraction yield of 9.99%. The successful synthesis of ZnO-NPs was confirmed by UV–Visible spectroscopy, which showed a characteristic absorption peak at 365 nm, while X-ray diffraction (XRD) analysis revealed a pure hexagonal wurtzite crystalline structure. FTIR spectroscopy further confirmed the interaction between the nanoparticle surface and the phytochemical compounds acting as capping agents. Antibacterial activity, evaluated using the agar well diffusion method, demonstrated that the biosynthesized ZnO-NPs exhibited broad-spectrum, concentration-dependent activity against *Staphylococcus aureus, Escherichia coli*, and *Pseudomonas aeruginosa,* with greater efficacy than the crude extract. Antioxidant activity assessed by the DPPH free radical scavenging assay showed a concentration-dependent increase in inhibition for both the extract and ZnO-NPs, with the nanoparticles displaying superior activity. A sunscreen cream containing the synthesized ZnO-NPs was successfully formulated and exhibited satisfactory sun protection factor (SPF) values and a stable pH compatible with skin physiology, supporting their potential application in the development of natural and effective sunscreen formulations.

Keywords: *Daucus carota L.*, zinc oxide nanoparticles, antibacterial activity, antioxidant activity, sun protection factor, sunscreen formulation.

تركيبة واقية من الشمس تعتمد على جزيئات أكسيد الزنك النانوية وبذور الجزر

الملخص

أدى الطلب المتزايد على مستحضرات الحماية من الأشعة فوق البنفسجية الطبيعية والفعالة إلى زيادة الاهتمام بالتوليف الأخضر للمواد النانوية ذات الأصل النباتي وتطبيقاتها في مجال مستحضرات التجميل. تهدف هذه الدراسة إلى التوليف الأخضر لجسيمات أكسيد الزنك النانوية (ZnO-NPs) باستخدام المستخلص المائي لبذور *Daucus carota L.* بوصفه عاملًا مختزلًا ومثبتًا حيويًا، وتقييم خصائصها البيولوجية وإمكاناتها في الحماية من الأشعة فوق البنفسجية. أظهر التحليل الفيتوكيميائي للمستخلص محتوى مرتفعًا من المركبات الفينولية، تلتها التانينات والفلافونويدات، بنسبة استخلاص بلغت 9.99%. وأكدت نتائج مطيافية الأشعة فوق البنفسجية–المرئية (UV–Vis) تكوّن جسيمات ZnO-NPs من خلال ظهور قمة امتصاص مميزة عند 365 نانومتر، كما أظهر تحليل حيود الأشعة السينية (XRD) بنية بلورية سداسية نقية من نوعWurtzite ، في حين أكد تحليل FTIRوجود تفاعل بين سطح الجسيمات النانوية والمركبات الفيتوكيميائية المغلفة لها. وأظهر اختبار النشاط المضاد للبكتيريا بطريقة الانتشار في الآبار على الأجار أن جسيمات ZnO-NPs المحضرة حيويًا تمتلك نشاطًا واسع الطيف ومعتمدًا على التركيز ضد *Staphylococcus aureus* و *Escherichia coli* و*Pseudomonas aeruginosa*، بكفاءة أعلى مقارنة بالمستخلص الخام. كما أظهر تقييم النشاط المضاد للأكسدة باستخدام اختبار DPPH زيادة تدريجية في نسبة التثبيط مع زيادة التركيز لكل من المستخلص والجسيمات النانوية، مع تفوق واضح لجسيمات ZnO-NPs. وتم تحضير كريم واقٍ شمسي يحتوي على الجسيمات النانوية المحضرة، وأظهر قيم SPF مرضية ودرجة حموضة مستقرة ومتوافقة مع فيزيولوجيا الجلد، مما يدعم إمكانية استخدامها في تطوير مستحضرات واقية شمسية طبيعية وفعالة.

الكلمات المفتاحية: *Daucus carota L*.، جسيمات أكسيد الزنك النانوية، مضاد للبكتيريا، مضاد للأكسدة، عامل الحماية من الشمس، كريم واقٍ شمسي.

Une formule de crème solaire à base de nanoparticules d'oxyde de zinc et de *(Daucus carrot. L)*

Résumé

La demande croissante en formulations naturelles et efficaces de protection contre les rayonnements ultraviolets (UV) a suscité un intérêt accru pour la synthèse verte de nanoparticules d'origine végétale destinées aux applications cosmétiques. Cette étude avait pour objectif la synthèse verte de nanoparticules d'oxyde de zinc (ZnO-NPs) à l'aide de l'extrait aqueux des graines de *Daucus carota L.*, utilisé comme agent réducteur et stabilisant, ainsi que l'évaluation de leurs propriétés biologiques et de leur potentiel photoprotecteur. L'analyse phytochimique a révélé une teneur élevée en composés phénoliques, suivis des tanins et des flavonoïdes, avec un rendement d'extraction de 9,99 %. La formation des ZnO-NPs a été confirmée par spectroscopie UV-Visible, mettant en évidence un pic d'absorption caractéristique à 365 nm, tandis que l'analyse par diffraction des rayons X (XRD) a révélé une structure cristalline hexagonale pure de type wurtzite. L'analyse FTIR a confirmé l'interaction entre la surface des nanoparticules et les composés phytochimiques jouant le rôle d'agents de stabilisation. L'activité antibactérienne, évaluée par la méthode de diffusion en puits sur gélose, a montré que les ZnO-NPs biosynthétisées présentaient une activité à large spectre dépendante de la concentration contre *Staphylococcus aureus*, *Escherichia coli* et *Pseudomonas aeruginosa*, avec une efficacité supérieure à celle de l'extrait brut. L'activité antioxydante, évaluée par le test de piégeage du radical libre DPPH, a montré une augmentation de l'inhibition en fonction de la concentration pour l'extrait et les ZnO-NPs, ces dernières présentant la meilleure activité. Une crème solaire contenant les ZnO-NPs synthétisées a été formulée avec succès et a présenté des valeurs de SPF satisfaisantes ainsi qu'un pH stable compatible avec la physiologie cutanée, soutenant ainsi leur potentiel pour le développement de formulations solaires naturelles et efficaces.

Mots-clés : *Daucus carota L.*, nanoparticules d'oxyde de zinc, activité antibactérienne, activité antioxydante, protection solaire, formulation de crème solaire.

List of figures

List of tables

Summary

Introduction

I. Introduction

Exposure to ultraviolet (UV) radiation represents one of the primary environmental factors responsible for cutaneous damage, encompassing sunburn, premature photoaging, and an elevated risk of skin cancer. As awareness of these harmful effects continues to grow, the demand for effective and safe sunscreen formulations has increased substantially. In parallel, there has been a marked shift in research interest toward natural and eco-friendly photoprotectiv preparations that combine UV-filtering efficacy with additional biological benefits such as antioxidant activity (Nikam et al., 2023).

Daucus carota L. seeds constitute a valuable botanical source of diverse bioactive phytochemicals, including phenolic compounds, flavonoids, tannins, and vitamins. These constituents are well recognized for their capacity to neutralize free radicals generated upon UV exposure and to mitigate oxidative stress-related skin injury. The notable phytochemical richness of carrot seed extract has therefore attracted considerable interest as a natural active ingredient in cosmetic and dermatological formulations.

Zinc oxide nanoparticles (ZnO-NPs) are among the most extensively employed inorganic UV filters in modern sunscreen products, offering broad-spectrum protection against both UVA and UVB radiation with excellent photostability and skin compatibility (Nikam et al., 2023). Beyond their photoprotective function, ZnO-NPs have demonstrated significant antibacterial and antioxidant properties, further broadening their potential in multifunctional cosmetic applications (Haiouani et al., 2024). The green synthesis of ZnO-NPs using plant extracts as biological reducing and stabilizing agents represents a sustainable and cost-effective alternative to conventional synthesis methods that often employ toxic chemicals (Mohamad Sukri et al., 2023). Phytochemicals present in plant extracts, including phenolic compounds, flavonoids, and terpenoids, act as bioreducing and stabilizing agents, and can modulate the size, shape, and crystallinity of the resulting nanoparticles, thereby influencing their biological functionality (Ansari et al., 2024).

In this context, the present study aims to biosynthesize ZnO nanoparticles using *Daucus carota L.* seed extract as a bio-reducing agent, and to evaluate their physicochemical, biological, and photoprotective properties. The investigation encompasses phytochemical characterization of the extract, structural characterization of the synthesized nanoparticles, assessment of antibacterial and antioxidant activities, and evaluation of the sun protection factor (SPF) and pH of a sunscreen cream formulation incorporating the biosynthesized ZnO-NPs.

Part1

Bibliography Synthesis

Chapitre01: Nano

I. The nano world

I.1. Nano science:

Nanoscience represents a fundamental field in modern chemistry, materials science, and biology. The development of techniques allowing the synthesis and manipulation of materials at the nanoscale has contributed significantly to advances in several domains, including catalysis, optical technologies, and biomedical applications. In addition, engineered nanomaterials such as nanocrystals and two-dimensional materials possess specific physicochemical properties that differ from those observed in bulk materials, leading to major progress in their synthesis, processing, and characterization. (Yang, S. 2025). Nanoscience is the study of the unique properties of materials between 1− 100 nm, and nanotechnology is the application of such research to create or modify novel objects. (SERJAY SIM. 2021)

I.1.2. Nano Technology:

Nanotechnology is an interdisciplinary field of science and engineering focused on the design, production, and application of materials and devices with dimensions ranging from 1 to 100 nanometers. At this scale, materials exhibit distinctive physical and chemical characteristics that differ significantly from those observed in their bulk form. These differences are mainly attributed to quantum mechanical effects and the increased influence of surface-related phenomena. Owing to these unique properties, nanotechnology has become a major area of interest in modern physics and has contributed to the emergence of nanophysics as an important scientific discipline.

Nanotechnology has considerably broadened the applications of modern physics by enabling precise manipulation of matter at the atomic and molecular scales. Nanostructured materials exhibit unique electrical, optical, and magnetic properties resulting from quantum confinement effects, surface phenomena, and enhanced interfacial interactions. Owing to these characteristics, such materials have found important applications in various fields, including energy technologies, medical physics, environmental monitoring, and space science, where conventional materials may present limited performance. (Rajiput, J 2025).

I.1.3. Nanomaterials:

Nanomaterials have attracted considerable scientific interest due to their wide range of potential applications in different fields. A nanometer represents an extremely small unit of length, corresponding approximately to the alignment of a few atoms, such as several silicon or hydrogen atoms arranged in a line. Materials are classified as nanomaterials when at least one of their dimensions falls within the nanoscale range, typically between 1 and 100 nm. (Nadeem Baig, 2021). And classification of nanomaterials in Figure 1 illustrates how nanomaterials can be divided into depending on their size, place of origin structural configuration, pore size, and potential toxicity. (MekuyeBirhanu Abera. 2023)

Nanomaterials are involved in numerous fields of application due to their unique properties and versatile functionalities. As presented in Table 1, they are widely used in nanomedicine through applications such as nanodrugs, medical devices, and tissue engineering. They are also employed in chemical and cosmetic industries, particularly in the formulation of nanoscale compounds, paints, coatings, and various advanced materials used in materials science. (MekuyeBirhanu Abera, 2023)

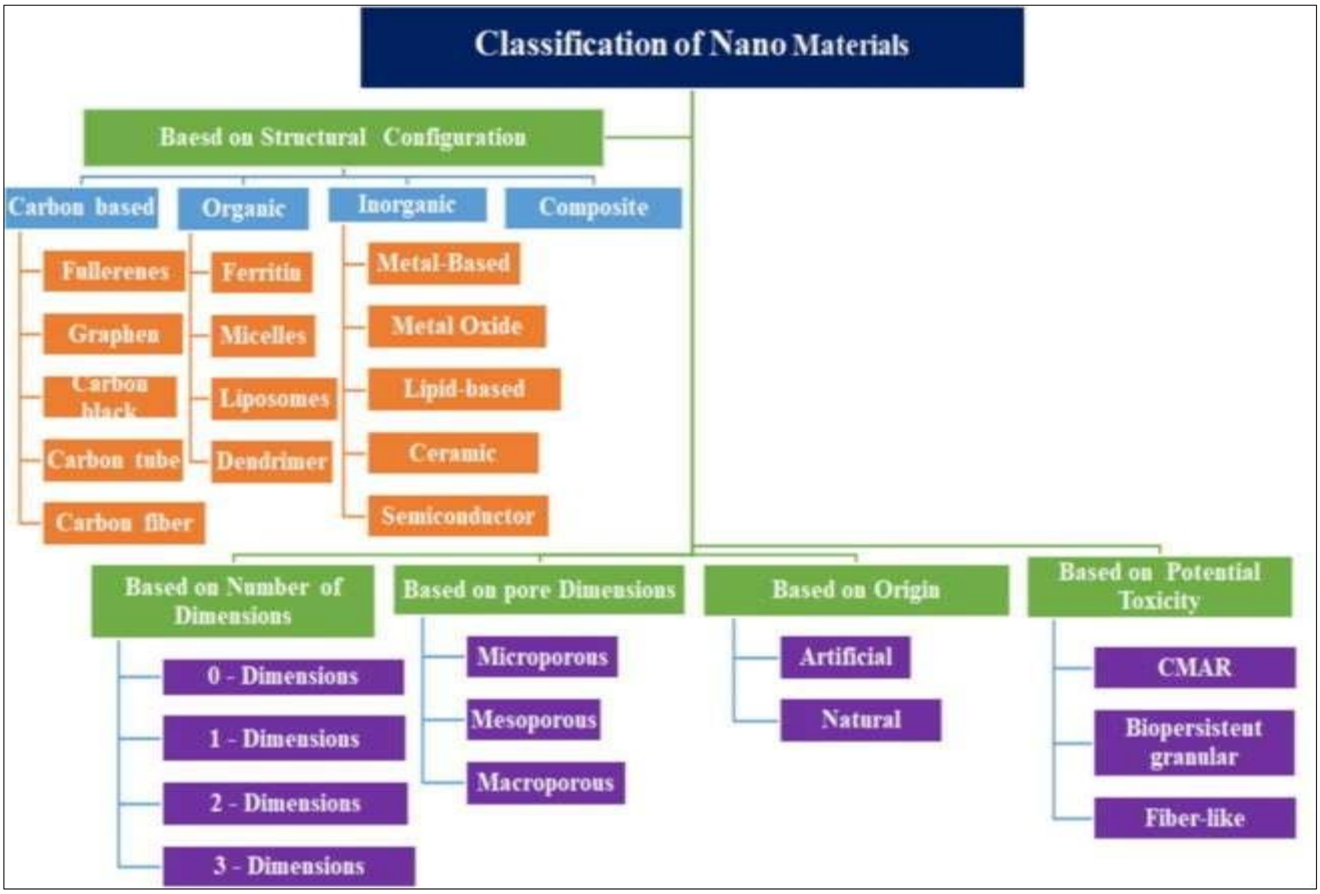

Figure1: Classification of nanomaterials.(Mekuye, B. 2023)

I.2. Nanoparticules

I.2.1. Physicochemical Properties of Nanomaterials and Nanoparticles

Nanoparticles possess unique physicochemical properties that differ significantly from those of the same materials in their bulk form. These distinctive characteristics arise from the reduction of material dimensions to the nanoscale, resulting in changes in surface structure, atomic interactions, and energy states. Consequently, nanoparticles have found widespread applications in various fields, including medicine, environmental science, electronics, and materials engineering, owing to their enhanced physical and chemical performances (Nadeem Joudeh, 2022).

The physical properties of nanomaterials are strongly influenced by their extremely small size and large surface area. As particle size decreases, the surface-to-volume ratio increases considerably, leading to a greater proportion of atoms being located on the particle surface. This phenomenon enhances surface energy and contributes to increased reactivity and mechanical strength. Furthermore, unlike bulk materials whose melting temperature remains constant, nanomaterials exhibit a reduction in melting point with decreasing particle size due to the presence of less tightly bound surface atoms. The increased surface area also promotes a tendency for nanoparticles to agglomerate in order to minimize surface energy (Mekuye, 2023).In addition to size-related effects, nanomaterials exhibit remarkable optical properties that are absent in their bulk counterparts. Their interaction with light can result in unique optical phenomena such as localized surface plasmon resonance (LSPR), which causes changes in color depending on particle size and morphology. Nanoparticles may also display specific abilities to absorb, transmit, or reflect visible and ultraviolet radiation. These characteristics make them particularly valuable in optical devices, sensors, coatings, and photoprotective applications (Nadeem Baig, 2021).

Several other physical properties contribute to the technological importance of nanoparticles. Their mechanical behavior, including elasticity, flexibility, ductility, and tensile strength, can be significantly improved at the nanoscale. Moreover, characteristics such as hydrophilicity, hydrophobicity, suspension stability, diffusion, and sedimentation behavior influence their performance in biological and industrial systems. Nanoparticles also exhibit important electrical, magnetic, and thermal properties, including conductivity, semiconductivity, resistivity, and enhanced thermal transport, which support their use in advanced electronic and sustainable energy technologies (Yousaf Khan, 2022).

The chemical properties of nanoparticles are equally important in determining their practical applications. Their high surface area and abundance of active sites increase their chemical reactivity and often provide enhanced catalytic performance compared with conventional bulk materials. Nanoparticles may exhibit improved catalytic activity, selectivity, and efficiency, making them valuable in chemical synthesis, environmental remediation, and industrial processes. Their behavior is also influenced by stability and sensitivity to environmental conditions such as temperature, light, moisture, and surrounding media (Mekuye, 2023).Another critical chemical characteristic is surface charge, commonly evaluated through zeta potential measurements. Surface charge governs the interactions between nanoparticles and their environment, influencing colloidal stability, dispersion behavior, and the tendency to aggregate. Nanoparticles with suitable surface charge values generally remain well dispersed in solution, whereas insufficient electrostatic repulsion can lead to agglomeration and reduced functionality (Nadeem Baig, 2021).

Furthermore, nanoparticles may possess specific biological and environmental activities, including antibacterial, antifungal, disinfectant, and toxic effects. Additional chemical parameters such as flammability, corrosiveness, anticorrosive behavior, oxidation potential, and reduction potential further determine their suitability for particular applications. These combined physicochemical characteristics make nanomaterials versatile and highly effective materials for a broad range of scientific and industrial purposes (Yousaf Khan, 2022).

I.2.2. Methods of Synthesizing Nanoparticles and Nanomaterials:

Table1: Summary of nano applications of nano-materials (Mekuye, B . 2023)

Field of application	Principles of application	Nanomaterials
Solar cell	Convert photon energy in to electricity	Ag NW, Cu NW
OLED	To emit light	ITO electrodes
Super capacitor	Very fast charger or discharger, high power storage	Lithium, sodium, potassium
Transistor	For amplifying or switching electrical power	Si & Ge
Lithium-ion batteries	Produce rechargeable batteries	Carbon nanotubes, nanosized transition metal oxide, nano-sized composite material
Imaging	Ability to penetrate cells, good analytical signals	Ag and Cu bimetallic nanoparticles
Cancer diagnosis	Biomedical Imaging Used for Cancer and tumor detection	Gold and iron-based nanoparticles
Drug delivery and cancer therapy	The aim of drug delivery includes precise targeting and therapeutic efficacy	Au nanoparticle, silicon nanoparticle, carbon nanotube, nano graphene
Biomedicine	Gene delivery	CNTs
COVID-19 diagnosis and Prevention	rSARS-CoV-2 tagging and development of COVID-19 mRNA vaccines	Lipid nanoparticles Au nanoparticle
Against monkey pox	Chelating the vires circulating in the blood stream. Block vires host cell binding and penetration	Iron oxide nanoparticle Ag nano particle
Medical	Selective reactivity with certain biomolecules and antiviral activity	Fullerenes
Food industry	Despite toxicological concerns, detect volatile organic compounds	TiO_2 and Ag
Agricultural	Fertilizer developer	SiO_2, ZnO, CuO, Fe, and Mg
Potential vaccine adjuvant	Used for the development of robust immune response.	Aluminum hydro-oxide, gold nanoparticle
Anti -bacterial activity	Used in treatment of disease caused by bacteria.	Gold, silver, copper, titanium, iron nanoparticle
High sensitivity sensor	For detecting varies parameters like electrical resistivity, magnetic permeability, thermal conductivity and capacitance	ZnSe, CdS, ZnS, CdTe
Data storage	The aim of this is to store a large amount of information	Spintronics & nanowires
Aero industry	To protect air craft from lighting strike	Cu Mesh
Electromagnetic interference shielding	Blocking EM radiation	Al, Cu, steel
Display	Resolution of the image on the monitor by reducing pixel size	CNTs
Micro-electronics	To produce faster logic gates	Carbon nanotube, lead telluride, cadmium sulphide
Construction	Increase the strength of material	SiO_2, Fe_2O_3
Cutting tools	For hard material	Tungsten carbide
Environmental	Increase growing rate of plants	CNTs
Elimination of pollutants	Used as catalysts to react with toxic gases	Titanium oxide, calcium carbonate mixed silicon-based polymer
Energy	Alternating energy storage media	CNTs
Textile	Coating textiles such as nylon, to provide antimicrobial characteristics	Ultra-hydrophobic water-resistant and strain resistance fabrics
Cosmetics	Used in sunscreen and in the cosmetic industry	Titanium oxide, zinc oxide
Car tires	Mechanical reinforcement	Carbon block
Car bumpers	To make car exterior lighter	Nanosized clay

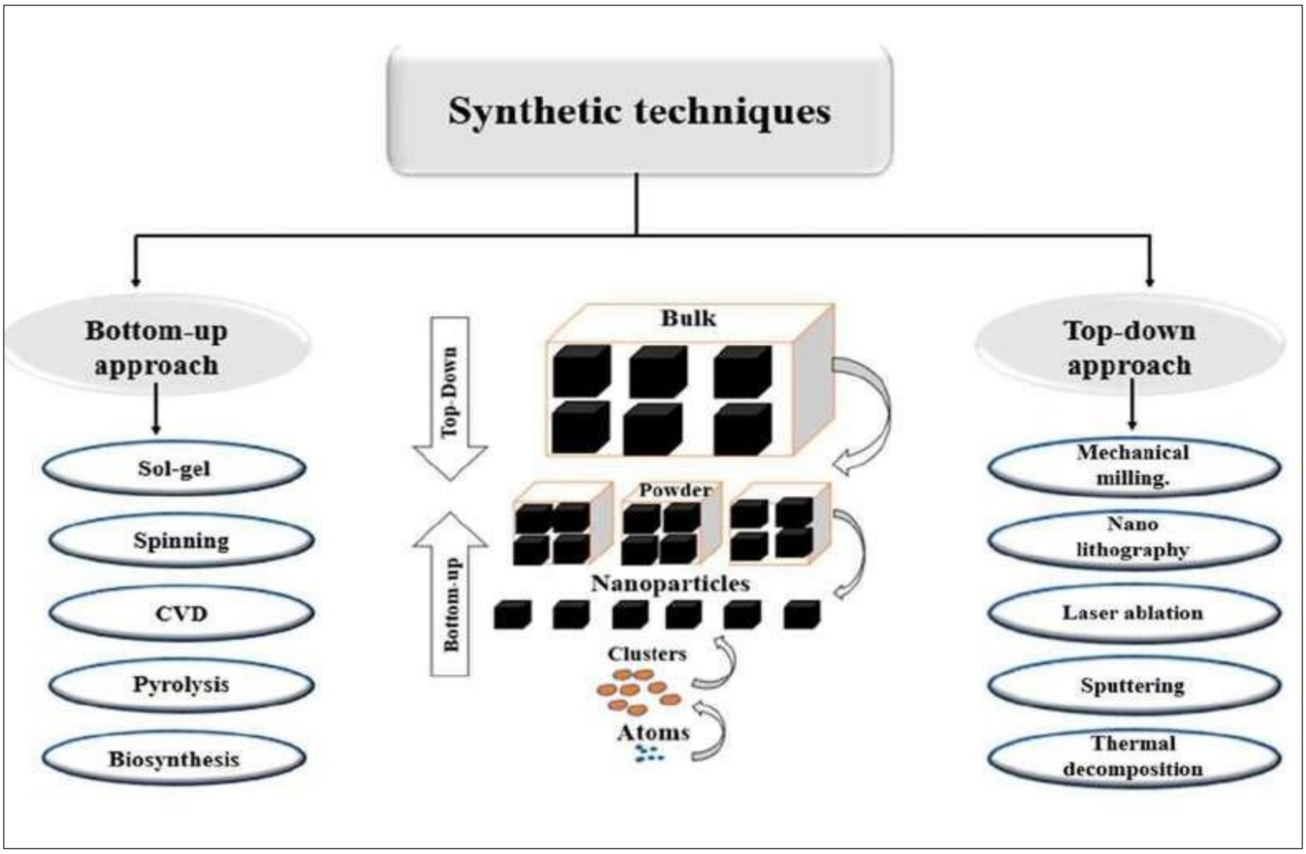

Figure2: Bottom-up and top-down synthetic approaches to nanoparticles (Khan, Y ET al2022.)

Nanomaterials are synthesized through a wide range of techniques that are generally classified into two main approaches: top-down and bottom-up methods. These approaches differ in their fundamental principles, level of control over nanoscale structures, and resulting material properties. The selection of a synthesis route significantly influences the physicochemical characteristics of nanoparticles such as size, morphology, stability, and surface reactivity (Mekuye, 2023; Nadeem Joudeh, 2022).

I.2.2.1. Top-Down Approaches

The top-down approach is a destructive fabrication strategy in which bulk materials are broken down into smaller structures until the nanoscale is reached. This method is conceptually similar to sculpting a solid block into a desired shape. It is widely used in industry due to its scalability and compatibility with large-area processing, although it often leads to broader particle size distribution and surface defects (Paras, 2023; Mekuye, 2023).

Top-down methods include several techniques such as lithography, mechanical milling, laser ablation, sputtering, arc discharge, and thermal decomposition. These methods are effective for mass production but generally provide limited atomic-level control over nanostructure formation (Yousaf Khan, 2022; Materials Advances Review, 2021).

I.2.2.1.1 Mechanical Milling

Mechanical milling is one of the most widely used top-down methods for nanoparticle production. It involves high-energy grinding of bulk materials using rotating balls inside a milling chamber, leading to repeated fracture and refinement of particles into nanoscale dimensions. This method is commonly used for producing nanoalloys and reinforced composites, particularly in metal-based systems (Materials Advances Review, 2021; Paras, 2023).

I.2.2.1.2 Nanolithography

Nanolithography is a patterning technique used to fabricate nanoscale structures by transferring designed patterns onto a substrate using light or electron beams. It allows precise control over nanoparticle geometry and arrangement. However, it requires complex instrumentation and is relatively expensive, which limits large-scale application (Materials Advances Review, 2021; Paras, 2023).

I.2.2.1.3 Laser Ablation

Laser ablation involves irradiating a target material with a high-energy laser beam, causing vaporization and formation of nanoparticles in a surrounding medium. It is considered a green synthesis method since it does not require chemical reducing agents. However, prolonged irradiation may reduce efficiency due to nanoparticle shielding effects (Yousaf Khan, 2022; Materials Advances Review, 2021).

I.2.2.1.4 Sputtering

Sputtering is a physical deposition technique in which energetic ions bombard a solid target, ejecting atoms that are deposited as thin nanostructured films on a substrate. The process allows high-purity coatings but has relatively low deposition rates and energy loss in the form of heat (Materials Advances Review, 2021; Paras, 2023).

I.2.2.1.5 Thermal Decomposition

Thermal decomposition is a method in which precursors are broken down at high temperatures, leading to nanoparticle formation. It is widely used for producing monodispersed nanoparticles with controlled size. However, it is limited by restricted precursor compatibility and difficulty in controlling complex compositions (Materials Advances Review, 2021; Yousaf Khan, 2022).

I.2.2.1.6 Arc Discharge Method

The arc discharge method is used for the synthesis of carbon-based nanomaterials such as fullerenes, carbon nanotubes, and graphene. It involves generating an electric arc between graphite electrodes under controlled atmospheric conditions. Although highly effective for carbon nanostructures, controlling purity and morphology remains challenging (Materials Advances Review, 2021; Yousaf Khan, 2022).

I.2.2.2. Bottom-Up Approaches

The bottom-up approach is a constructive method in which nanomaterials are built from atomic or molecular units through chemical or physical interactions. This strategy is inspired by natural biological systems where self-assembly plays a key role in forming complex structures. Bottom-up methods generally provide better control over size, morphology, and composition compared to top-down techniques (Mekuye, 2023; Nadeem Baig, 2021).

I.2.2.2.1 Sol–Gel Method

The sol–gel process involves the transformation of a colloidal solution into a gel network through hydrolysis and condensation reactions of metal precursors. It is widely used for synthesizing metal oxides and ceramic nanomaterials. This method offers advantages such as low processing temperature and high compositional uniformity, although it is sensitive to reaction conditions (Materials Advances Review, 2021; Nadeem Baig, 2021).

I.2.2.2.2 Spinning Method

The spinning disc reactor method produces nanoparticles by rapidly rotating a disc to enhance mixing of precursor solutions. This leads to controlled nucleation and particle formation under adjustable parameters such as temperature, flow rate, and rotation speed. It is suitable for continuous nanoparticle production (Paras, 2023; Materials Advances Review, 2021).

I.2.2.2.3 Chemical Vapor Deposition (CVD)

Chemical vapor deposition involves the reaction of gaseous precursors on a heated substrate to form thin films or nanostructures. It is widely used due to its ability to produce high-purity materials. However, it requires high temperatures and careful handling of gaseous precursors, which may be toxic or reactive (Materials Advances Review, 2021; Paras, 2023).

I.2.2.2.4 Pyrolysis

Pyrolysis is a thermal decomposition process used for large-scale production of nanoparticles. It is simple, continuous, cost-effective, and suitable for industrial applications. However, particle aggregation after formation can affect size uniformity (Materials Advances Review, 2021).

I.2.2.2.5 Hydrothermal and Solvothermal Methods

These methods involve chemical reactions under high temperature and pressure in sealed systems. They are widely used to produce nanostructures such as nanorods, nanowires, and nanosheets. They allow good control over morphology but require specialized equipment (Materials Advances Review, 2021; Nadeem Joudeh, 2022).

I.2.2.2.6 Soft and Hard Templating Methods

Templating methods use structured materials to guide nanoparticle formation. Soft templates involve surfactants and self-assembled molecules, while hard templates use rigid materials such as silica or carbon. These methods enable precise control of pore size and nanostructure formation (Materials Advances Review, 2021; Nadeem Baig, 2021).

I.2.2.2.7 Reverse Micelle Method

Reverse micelles act as nanoscale reactors formed in water-in-oil systems. The nanoparticle size can be controlled by adjusting the water-to-surfactant ratio. This method produces uniform and monodispersed nanoparticles (Materials Advances Review, 2021).

I.2.2.2.8 Biosynthesis (Green Synthesis)

Biosynthesis uses biological organisms such as bacteria, fungi, algae, and plant extracts to produce nanoparticles in an eco-friendly way. Biomolecules act as reducing agents, enabling safe synthesis for biomedical applications. However, purification challenges and variability in biological systems remain limitations (Yousaf Khan, 2022; Materials Advances Review, 2021).

I.2.2.2.9 Molecular Self-Assembly

Molecular self-assembly is a spontaneous process in which molecules organize into ordered nanostructures through non-covalent interactions. It is driven by a balance of attractive and repulsive forces and is widely used to fabricate highly ordered nanomaterials in the 1–100 nm range (Nadeem Baig, 2021).

I.2.2.3. Comparison of Top-Down and Bottom-Up Approaches

Top-down methods are generally simpler, cost-effective, and suitable for large-scale production, but they often suffer from broad size distribution and structural defects. In contrast, bottom-up methods provide better control over particle size, shape, and composition, enabling the fabrication of highly uniform nanomaterials. However, they may require more complex reaction conditions and precise control of synthesis parameters (Paras, 2023; Mekuye, 2023).

I.2.3. Characterization of nanoparticule :

The potential and use of nanoparticles are both determined by the qualities that make it distinct.
(Yousaf khan,2022)

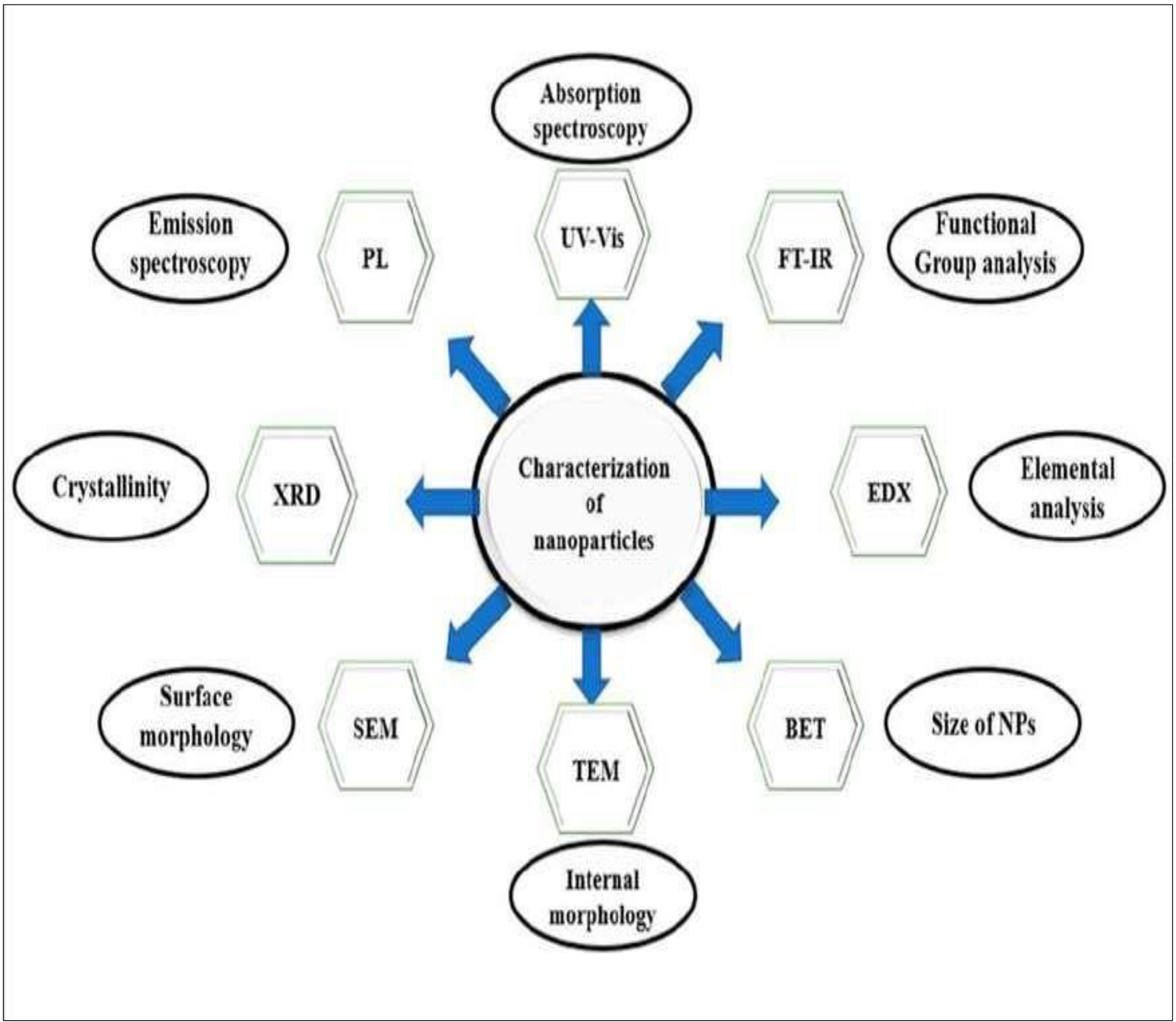

Figure3: Overview of characterization of nanoparticule. . (Yousaf khan,2022)

I.2.3.1. X-ray Diffraction (XRD):

X-ray diffraction (XRD) is a widely employed analytical technique for investigating the structural properties of nanomaterials. It operates on the principle of elastic scattering of X-rays by the periodic arrangement of atoms in a crystalline lattice. The interaction between the incident beam and the crystal planes results in constructive interference, producing a characteristic diffraction pattern that reflects the internal structure of the material. This pattern is governed by parameters such as the X-ray wavelength, diffraction angle, and interplanar spacing. (Paras, 2023; Nuha Al-Harbi, 2024)

This technique is extensively used for the characterization of nanomaterials in crystalline, amorphous, and polycrystalline forms. It enables the determination of several key properties, including phase composition, degree of crystallinity, lattice structure, internal strain, and estimation of crystallite size and morphology. The obtained diffraction patterns can be matched with standard reference databases to accurately identify the phases and composition of the studied sample. (Paras, 2023; Nuha Al-Harbi, 2024)

The fundamental principle governing XRD analysis is Bragg’s law, which defines the relationship between the diffraction angle and the crystal lattice spacing, as expressed in Equation (1):

$$2d \sin\theta = n\lambda \quad (1)$$

n = ordre de diffraction

λ(Å)= longueur d’onde des rayons X

d = distance inter réticulaire

θ (°) = angle de Bragg. . (Sabrina,H . 2023).

where d represents the interplanar distance, θ is the angle of incidence, λ is the wavelength of the X-rays, and n denotes the order of reflection. This equation is essential for interpreting diffraction data and determining the crystalline structure of materials. (Paras, 2023; Nuha Al-Harbi, 2024)

Moreover, the crystallite size of nanoparticles can be estimated using the Debye–Scherrer equation, shown in Equation (2):

$$D = k\lambda / (\beta \cos\theta) \quad (2)$$

where D is the crystallite size, k is the Scherrer constant (0.94), β is the full width at half maximum (FWHM), and θ is the diffraction peak position. This relationship is commonly applied for size estimation of nanomaterials based on XRD peak broadening. (Paras, 2023; Nuha Al-Harbi, 2024)

I.2.3.2. Ultraviolet–Visible (UV–Vis) Spectroscopy:

Ultraviolet–Visible (UV–Vis) spectroscopy is an analytical technique used for the characterization and compositional analysis of substances and nanoparticles. It is considered a simple, rapid, and cost-effective method. Its principle is based on measuring the intensity of light absorbed or reflected by a sample and comparing it with a reference material, which allows the evaluation of the optical response of the investigated system. (Paras, 2023)

UV–Vis spectroscopy is also widely used to confirm nanoparticle formation through the analysis of absorption spectra. The recorded spectral features provide important information about the transport and absorption properties of the sample, which are directly related to nanoparticle synthesis and behavior in colloidal systems. (Paras, 2023)

In addition, this technique is essential for determining key physicochemical properties of nanoparticles such as optical characteristics, refractive index, particle size, shape, and colloidal stability. For example, a characteristic shift in the maximum absorption wavelength from around 300 nm for $Zn(NO_3)_2$ to approximately 340–370 nm indicates its transformation into nano-zinc oxide. Furthermore, absorption bands around 300 nm are associated with π–π* transitions of C–C aromatic bonds, while shoulders near this region correspond to n–π* transitions of C=O bonds. UV–Vis spectroscopy can also be used to verify the presence, functional state, and dispersion of graphene in different solvents such as ethanol, 1-propanol, ethylene glycol, and tetrahydrofuran. However, a limitation of this technique is that sample analysis can be time-consuming. (Nuha Al-Harbi, 2024)

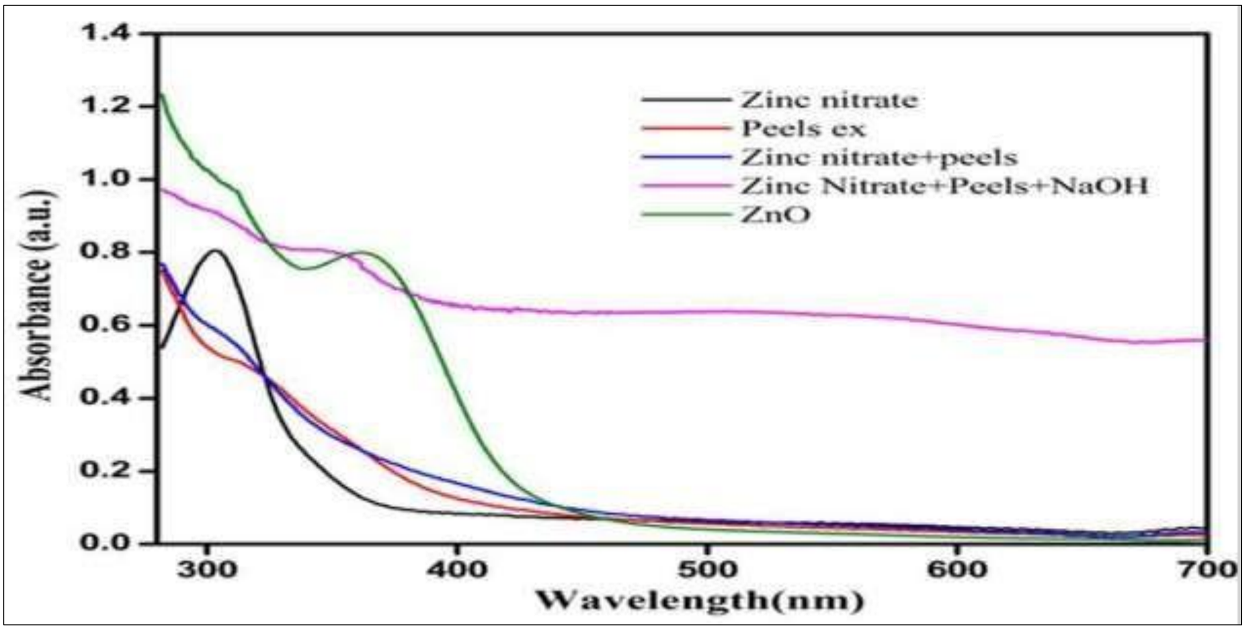

Figure4: UV–Vis absorption spectra and wavelength of Zn (NO3)2 nanoparticle

Principle

This technique is used to quantify the amount of UV or visible light absorbed by components in solution. It then measures the ratio between the intensities of the incident and transmitted light beams in the UV–Visible region (Sabrina, H., 2023).

The absorption laws apply to ultraviolet, visible, and even infrared absorption spectra. This law is expressed by the following equation:

$$A = \log I / I0 = \text{s}.\ L\ .\ C$$

Where:

A: Absorbance

I_0 : Intensity of the incident light beam

I: Intensity of the transmitted light beam

L: Path length of the analytical cuvette

ε: Proportionality constant

C: Concentration of the absorbing substance.

I.2.3.3. Fourier Transform Infrared (FTIR) Spectroscopy:

Fourier Transform Infrared (FTIR) spectroscopy is a widely used analytical technique for investigating inorganic and organic molecular bonding. It is based on the interaction between infrared radiation and molecular vibrations within a sample. The infrared region typically covers wavelengths from 700 nm to 1 mm, corresponding to the red end of the electromagnetic spectrum. When a sample is exposed to infrared radiation, it absorbs specific frequencies depending on its chemical bonds, generating a characteristic molecular fingerprint that reflects its composition and structure. This technique provides important qualitative information regarding the nature and components of the analyzed material. (Nuha, 2024)

FTIR spectroscopy is also a powerful method for identifying and analyzing functional groups in molecular structures. It operates within the infrared spectral range of approximately 4000 cm^{-1} to 400 cm^{-1}, which is commonly used for material characterization. The technique allows the detection of surface functional groups and provides insight into the optical and chemical properties of samples. In nanomaterials, FTIR is particularly useful for determining surface reactive sites and confirming interactions between nanoparticles and biological molecules through characteristic spectral band shifts. (Paras, 2023)

Figure 5: FTIR spectroscopy ATR

FTIR spectroscopy is further applied to study molecular vibrations within the range of 4000 cm^{-1} to 400 cm^{-1}, where different functional groups exhibit specific absorption bands. The spectrum is typically divided into the functional group region and the fingerprint region, each providing structural information about the compound. These vibrational modes depend on bond strength, atomic mass, and molecular environment, allowing detailed structural interpretation of complex materials, including powders, liquids, and thin films. (Sahra, 2023 & Ibrahim, 2020)

I.2.3.4. Synthesis of Nanoparticul Using Green Chimestry:

A). Carrot seed

The seeds are elliptical, albuminous diachenes containing flavonoids, polyphenols, and an essential oil composed of asarone, carotol, pinene, limonene, sesquiterpenes, and β-bisabolene. The seeds contribute to the reduction of oxidative stress and have shown a significant reduction in total cholesterol, triglycerides, and HDL and VLDL levels (Sing et al., 2010).

Among the plant materials explored for the green synthesis of nanoparticles, carrot seeds (*Daucus carota L.*) have emerged as a particularly promising and underexplored biological resource. As a member of the Apiaceae family, D. carota is widely cultivated across temperate and subtropical regions worldwide, making its seeds readily accessible, economically viable, and suitable for large-scale sustainable applications (Ismail et al., 2024)

The seeds of *Daucus carota* are notably rich in a diverse array of bioactive phytochemicals, including phenolic acids, flavonoids, terpenoids, and essential oil constituents such as carotol, limonene, and α-pinene (Ismail et al., 2024; Riaz et al., 2023). These compounds are of particular relevance in the context of green nanotechnology, as phytochemicals present in plant extracts — most notably flavonoids, phenolics, alkaloids, and terpenoids — function simultaneously as reducing agents, capping agents, and stabilizing agents during nanoparticle formation, facilitating controlled particle growth without the need for toxic chemical reagents (Frontiers in Nanotechnology, 2025; ScienceDirect, 2025).

B). Chemical composition of carrot seed:

Carrot seeds are characterized by a rich and diverse chemical composition, containing more than 310 bioactive compounds, including terpenoids, flavonoids, phenolic acids, and phenylpropanoids. This chemical diversity is distributed among 13 subspecies of wild carrot, contributing to the seeds' wide range of therapeutic properties, such as anti-inflammatory, antimicrobial, and anticancer activities (Ismail et al., 2024).

Carrot seeds contain four major groups of phytochemicals: phenolic compounds, carotenoids, polyacetylenes, and ascorbic acid. Among these, polyacetylenes such as falcarinol and falcarindiol are considered the most important bioactive compounds present in the seeds owing to their significant anti-inflammatory and anticancer properties through the inhibition of cancer cell proliferation (Ahmad et al., 2019).Several studies have demonstrated that the maturity stage of carrot seeds has a direct impact on their chemical composition and biological activity. The concentration of bioactive compounds reaches its maximum level at full maturity. Therefore, harvesting seeds at the fully mature stage is recommended to obtain the highest content of active constituents and the strongest antioxidant activity (Cvetković et al., 2023).

C). Use Of Carrot Seed:

Carrot seeds (*Daucus carota L.*) have been widely used in traditional medicine since ancient times due to their diverse therapeutic properties. They are known for their diuretic, carminative, antiseptic, and anti-inflammatory effects and have traditionally been used in the treatment of urinary calculi, cystitis, gout, and prostatitis (Ismail et al., 2024). Modern studies have further supported these traditional applications by demonstrating their effectiveness against infections, inflammation, and certain types of cancer (Ismail et al., 2024).In addition to their traditional uses, carrot seeds exhibit a broad range of pharmacological activities, including antioxidant, analgesic, antimicrobial, antifungal, hepatoprotective, nephroprotective, antispasmodic, and anticancer properties (Deshmukh et al., 2021).

Moreover, the absence of serious adverse effects following their consumption highlights their potential safety for therapeutic applications (Deshmukh et al., 2021).Carrot seeds are also an important source of bioactive compounds for pharmaceutical and cosmetic industries. They are used to obtain essential oils, fixed oils, extracts, and purified compounds, particularly carotenoids (Kulawik-Pióro, 2022). These products are widely incorporated into cosmetic formulations because of their antioxidant, skin-repairing, and anti-aging properties, making them valuable ingredients in skincare and personal care products (Kulawik-Pióro, 2022).

Green synthesis is a sustainable approach derived from the principles of green chemistry, which aims to design chemical products and processes that reduce or eliminate the use and generation of hazardous substances. In nanoparticle synthesis, this approach focuses on producing functional nanomaterials while minimizing waste generation and environmental impact. Natural resources such as plant extracts, sugars, vitamins, and agricultural wastes are commonly used as reducing, stabilizing, and capping agents during nanoparticle formation. One of the earliest examples of green nanoparticle synthesis involved the use of D-glucose as a reducing agent and starch as a capping agent for silver nanoparticles (Medani, 2022).

Compared with conventional physical and chemical methods, green synthesis is considered safer, non-polluting, environmentally friendly, and more sustainable because it avoids the use of toxic chemicals and reduces the production of hazardous by-products. However, challenges such as long reaction times, limited availability of some biological raw materials, and difficulties in controlling particle size and product quality may affect the efficiency of the process (Ayub, 2025).Green-synthesized nanoparticles have gained significant attention due to their wide range of applications in cosmetic, food, agricultural, biomedical, electronic, and sensor-related fields. Their eco-friendly nature and diverse functional properties make them promising materials for industrial and technological applications (Sexina, 2025).

D). Green synthetisis (biosynthesis mecanisme):

The biosynthesis of nanoparticles is primarily based on the ability of bioactive phytochemicals, such as polyphenols, flavonoids, terpenoids, and lignans, to reduce metal ions into their elemental form. The resulting metal atoms aggregate to form small nuclei that serve as centers for nanoparticle growth. As the reduction process continues, additional atoms are deposited on these nuclei, leading to the formation of nanoparticles. Simultaneously, biomolecules present in the plant extract adsorb onto the nanoparticle surface and act as capping and stabilizing agents, preventing excessive aggregation and improving particle stability (Miu & Dinischiotu, 2022).

The biosynthetic process generally involves three main stages: reduction, nucleation, and growth, followed by stabilization of the formed nanoparticles. The efficiency of these stages is influenced by several factors, including the nature of the reducing agents, plant extract concentration, pH, and temperature, which affect the size, morphology, and physicochemical properties of the synthesized nanoparticles (Khan et al., 2022).In the case of metal oxide nanoparticles, such as zinc oxide (ZnO), metal ions may initially interact with functional groups present in plant biomolecules to form intermediate compounds. These intermediates are subsequently converted into metal oxide nanoparticles during drying or thermal treatment. Plant extracts therefore play a dual role as both reducing and stabilizing agents, making the biosynthesis process a simple and environmentally friendly approach for nanoparticle production (Miu & Dinischiotu, 2022; El-Seedi et al., 2019).

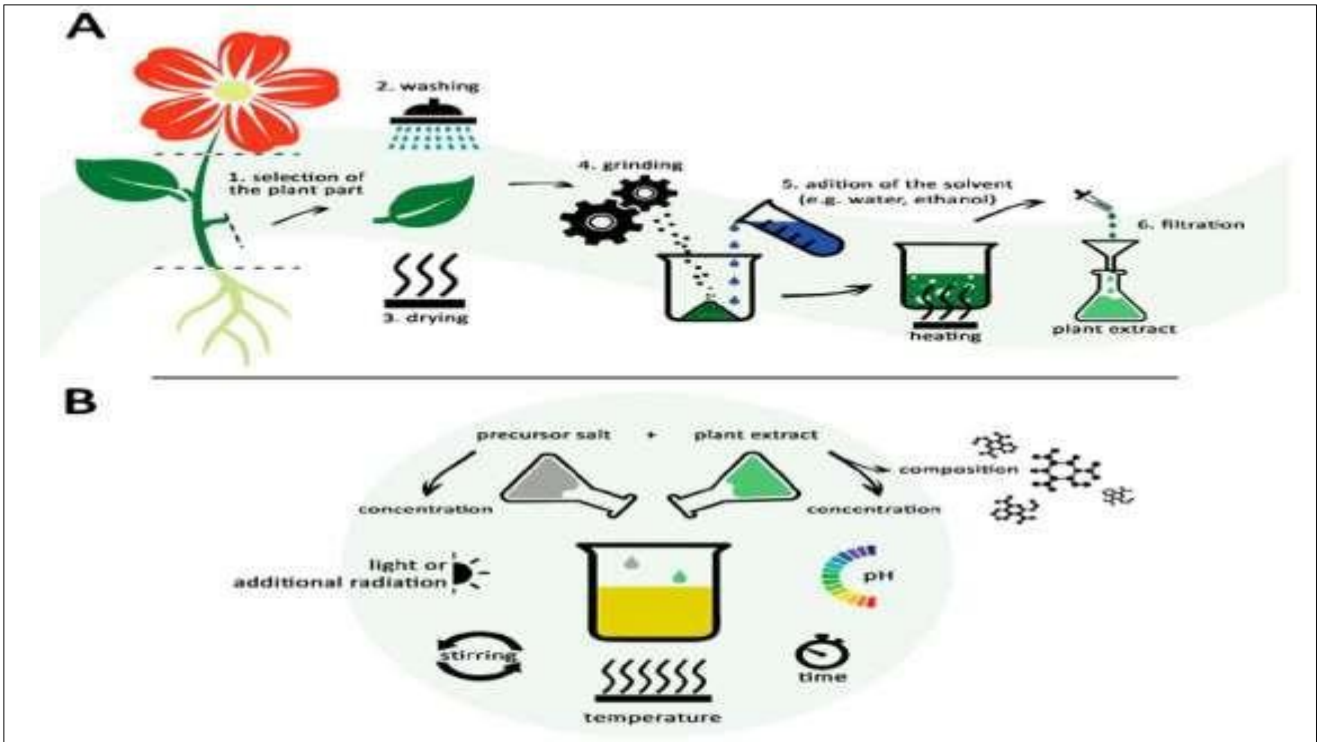

Figure 6. The typical approach of green synthesis of NPs: (A) Preparation of the plant extract; (B) factors affecting the reaction of green synthesis and the characteristics of the resulted NPs.(Miu, B., & Dinischiotu, A. 2022).

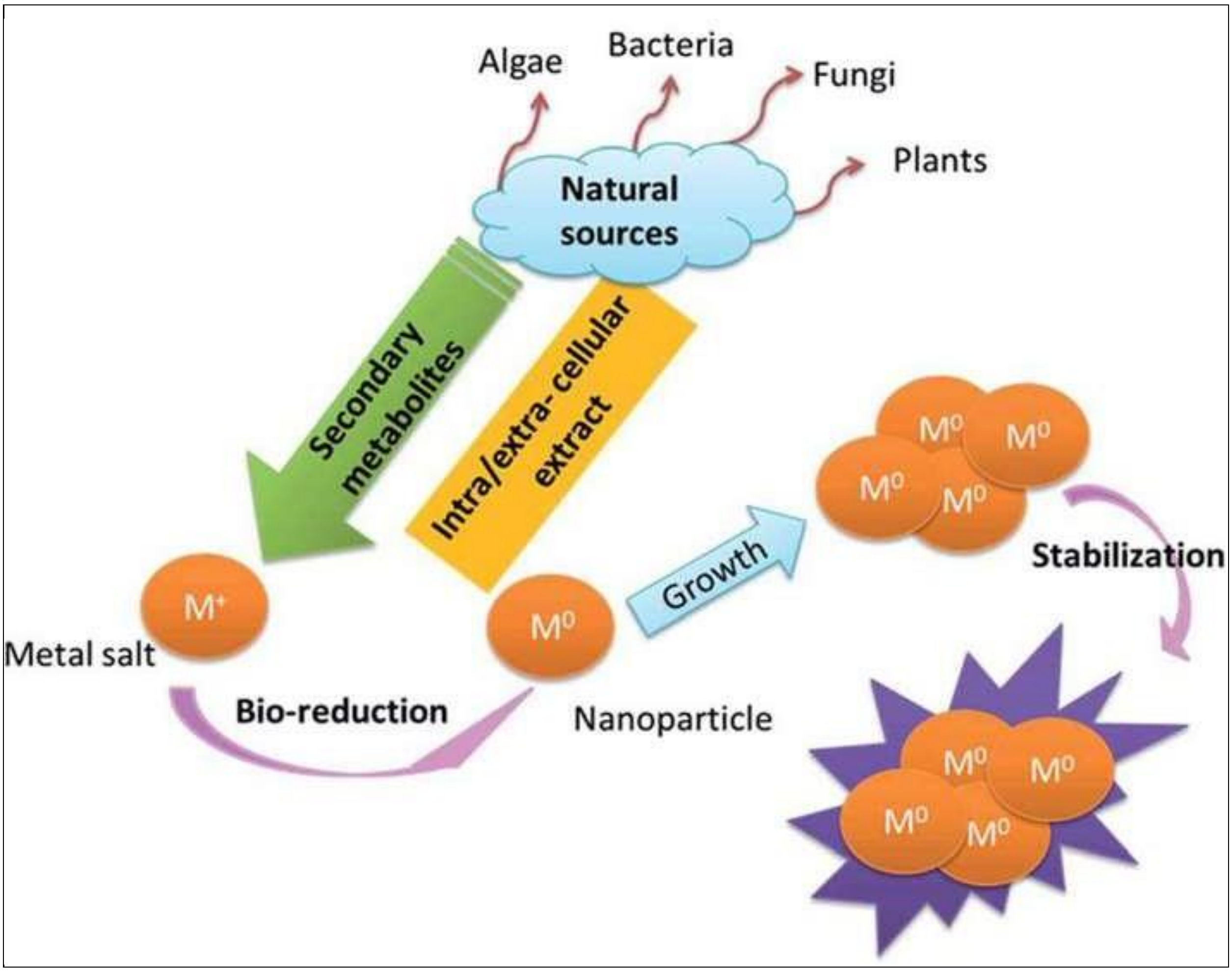

Figure7: Suggested general mechanisms for the synthesis of NPs(El-Seedi, H et al.2019)

Chapter 02 : Zinc oxide

I.3. Zinc oxide

I.3.1. Field of application for zinc oxide:

Zinc oxide nanoparticles (ZnO-NPs) have attracted considerable scientific attention over the past two decades owing to their distinctive physicochemical profile. Their combination of semiconducting behaviour, inherent biocompatibility, and potent antimicrobial activity positions them as one of the most studied nanomaterials in contemporary research (Mandal et al., 2022; Sayeem et al., 2026). The sections below survey their principal application domains, ranging from clinical medicine to precision agriculture.

I.3.1.1. Healthcare and Biomedical Applications

The United States Food and Drug Administration classifies zinc oxide as generally recognised as safe (GRAS), a status that has encouraged its adoption across multiple clinical contexts (Mandal et al., 2022).

a. Antimicrobial and Antiviral Activity

One of the most extensively documented properties of ZnO-NPs is their capacity to inhibit a wide range of pathogenic microorganisms, including bacteria, fungi, and several clinically relevant viruses such as influenza, herpes simplex, respiratory syncytial virus, and members of the coronavirus family (Sportelli et al., 2022; Mandal et al., 2022). This broad-spectrum efficacy has driven their integration into wound dressings — particularly for chronic wounds such as diabetic ulcers — as well as into antimicrobial coatings for personal protective equipment (Mandal et al., 2022).

b. Oncological Applications

In the field of cancer research, ZnO-NPs have been explored as photosensitisers capable of generating reactive oxygen species upon UV irradiation, thereby inducing selective cytotoxicity in tumour cells. Beyond photodynamic therapy, they have been shown to potentiate conventional chemotherapeutic agents and have been investigated within theranostic platforms that integrate diagnostic and therapeutic functions (Mandal et al., 2022).

c. Drug and Gene Delivery

The surface chemistry of ZnO nanoparticles can be tailored to enable controlled release of therapeutic payloads, making them attractive candidates for targeted drug delivery. Notably, certain formulations have demonstrated an ability to circumvent multidrug resistance mechanisms in cancer cell lines, which represents a significant translational challenge in oncology (Mandal et al., 2022).

d. Vaccine Adjutancy and Orthopedic Uses

ZnO-NPs have been evaluated as immunomodulatory adjuvants that may enhance antigen presentation in experimental vaccine systems (Vyas, 2020; Mandal et al., 2022). Separately, their incorporation into coatings for orthopaedic implants has been shown to simultaneously reduce bacterial colonisation, limit corrosion, and promote osteogenic differentiation — properties of considerable interest in reconstructive surgery (Mandal et al., 2022).

e. Broader Therapeutic Potential

Emerging evidence suggests that ZnO-NPs may also exert antioxidant, antidiabetic, cardioprotective, and antiparasitic effects, although most of this work remains at the preclinical stage and warrants further investigation before clinical translation can be considered (Mandal et al., 2022).

I.3.1.2. Environmental Remediation

a. Water and Air Treatment

As a photocatalyst, zinc oxide efficiently mineralises organic pollutants — including synthetic dyes and pharmaceutical micropollutants — under irradiation, while its surface affinity for heavy-metal ions enables adsorptive removal from contaminated matrices (Baig et al., 2025; Sayeem et al., 2026).

Analogous photocatalytic mechanisms underpin its use in air purification systems, where ZnO-based materials decompose volatile organic compounds and inactivate airborne pathogens (Baig et al., 2025).

b. Soil Remediation and Hydrogen Production

Application of ZnO-NPs to contaminated soils has been shown to immobilise heavy metals, reducing their bioavailability to plant and animal species (Sayeem et al., 2026). In the energy sector, the material's favourable band-gap characteristics make it a candidate for photocatalytic water splitting aimed at sustainable hydrogen generation (Baig et al., 2025; Vyas, 2020).

I.3.1.3. Industrial and Electronics Applications

a. Electronics and Energy Storage

The wide band gap and high electron mobility of ZnO underlie its established role in transparent conductive films, light-emitting diodes, laser devices, and thin-filmtransistors (Vyas, 2020). In energy storage, ZnO-NP incorporation has been reported to improve charge-transport kinetics in solar cells, batteries, and supercapacitors (Vyas, 2020; Sayeem et al., 2026).

b. Sensing, Textiles, and Food Packaging

ZnO-based sensors exhibit high sensitivity and rapid recovery characteristics that make them suitable for detecting trace gases and biological analytes (Vyas, 2020). In the textile industry, nanoparticle functionalisation imparts antimicrobial, UV-blocking, self-cleaning, and flame-retardant performance to fabrics (Sayeem et al., 2026). More recently, active food packaging incorporating ZnO-NPs has shown promise in extending product shelf life by suppressing microbial growth without compromising food quality (Sayeem et al., 2026).

I.3.1.4. Cosmetics and Personal Care

Physical sunscreens relying on ZnO as the active ingredient provide simultaneous protection against both UVA and UVB radiation, and the material's tolerability profile has encouraged its use in a variety of skincare preparations targeting acne, photoageing, and general skin barrier support (Vyas, 2020; Sayeem et al., 2026). In oral hygiene, ZnO-containing formulations have been shown to inhibit cariogenic bacteria, reduce dental plaque accumulation, and control oral malodour (Sayeem et al., 2026).

I.3.1.5. Agricultural Applications

The agricultural sector has begun to exploit ZnO-NPs as nanofertilisers that enhance micronutrient bioavailability and stimulate crop productivity at application rates substantially lower than those of conventional zinc fertilisers (Sayeem et al., 2026). Their antifungal and antimicrobial properties have also been harnessed in nanopesticide formulations designed to protect crops from phytopathogenic organisms with a reduced environmental footprint relative to synthetic agrochemicals. Additionally, ZnO-based nanomaterials are being incorporated into soil amendment and irrigation systems to improve water retention and overall water-use efficiency (Sayeem et al., 2026)

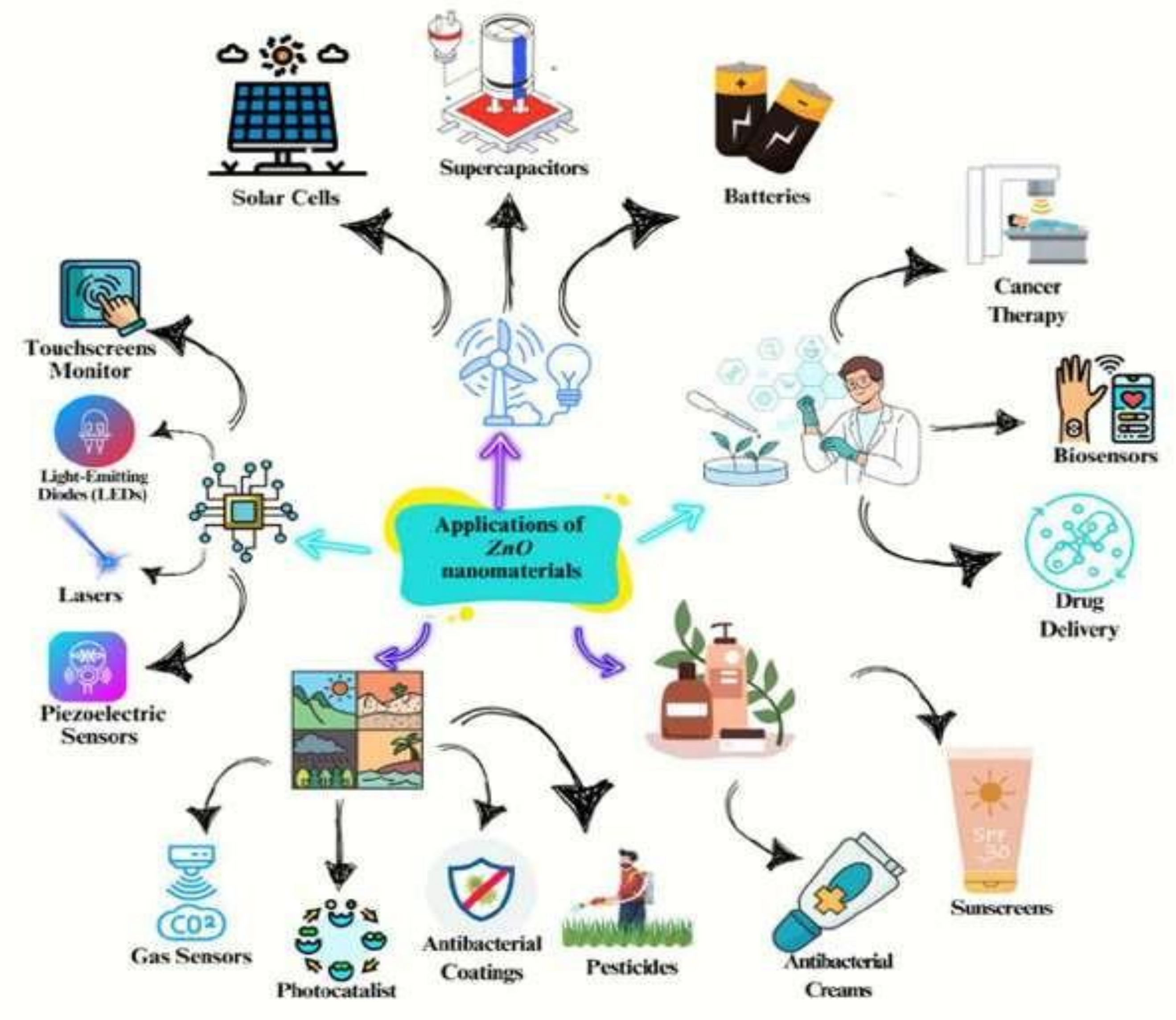

Figure 8: Illustration of the applications of ZnO NPs(nafis 2026)

I.3-2-Physicochemical Properties of Zinc Oxide:

Zinc oxide (ZnO) stands out among inorganic semiconductors as a material of remarkable versatility. Its unique combination of physicochemical, optical, and electronic properties has driven growing interest across multiple disciplines, spanning electronics, optoelectronics, sensing technologies, biomedical applications, and photocatalysis (Borysiewicz, 2019; Vyas, 2020).

In its most familiar form, ZnO appears as a white, odorless powder with a density of around 5.61 g/cm³. The material withstands high temperatures well, melting at approximately 1975 °C and boiling near 2360 °C. Under neutral conditions, ZnO dissolves poorly in both water and alcohols; however, exposure to acidic environments considerably accelerates its dissolution (Tereshkov et al., 2022; Sayeem et al., 2026).The properties of ZnO are deeply tied to its crystal structure. Three polymorphic forms are known: hexagonal wurtzite, cubic zinc-blende, and cubic rock-salt. Of these, wurtzite is by far the most stable phase at ambient conditions and the one most commonly encountered. Its non-centrosymmetric arrangement of atoms gives rise to piezoelectric and pyroelectric behavior, qualities that have made ZnO a favored material in electromechanical and sensing devices (Borysiewicz, 2019; Sayeem et al., 2026). The zinc-blende phase, being metastable, requires carefully controlled growth conditions to form, while the rock-salt structure emerges only under extreme pressures above 10 GPa (Borysiewicz, 2019; Ayoub et al., 2022).

Chemically, ZnO behaves as an amphoteric oxide, reacting with both acidic and basic media. This dual reactivity broadens its utility across industrial and environmental contexts (Tereshkov et al., 2022). At the nanoscale, ZnO particles develop high surface energy and abundant reactive surface sites, which enhance both their adsorption capacity and overall chemical reactivity. These same features, however, promote agglomeration, a tendency that must be carefully managed in practical applications (Valtsifer et al., 2023; Sayeem et al., 2026).From an electronic standpoint, ZnO is classified as a direct wide-bandgap semiconductor, with a bandgap of roughly 3.37 eV at room temperature. This relatively large bandgap makes the material transparent across the visible spectrum while conferring strong UV absorption, properties well-suited to UV photodetectors and optoelectronic systems (Vyas, 2020; Borysiewicz, 2019).

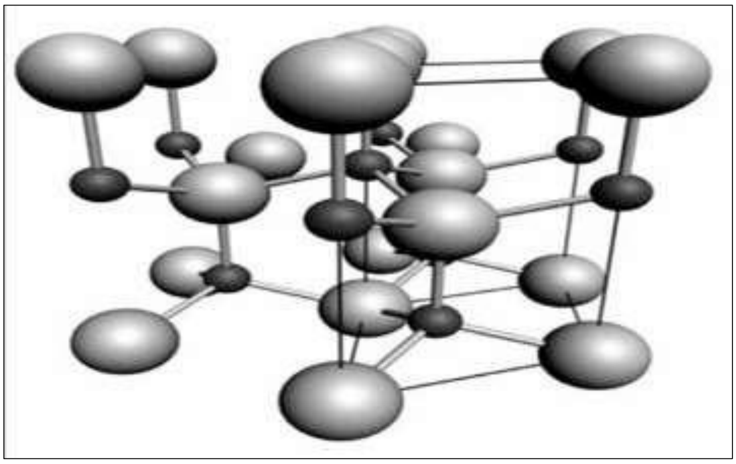

Figure9: The hexagonal wurtzite structure of ZnO (Ayoub,I et al . 2022)

Complementing this, ZnO possesses an exciton binding energy of about 60 meV, high enough to sustain excitonic emission at room temperature and thus support light-emitting device applications (Vyas, 2020; Ayoub et al., 2022).ZnO also exhibits intrinsic n-type electrical conductivity, a characteristic generally linked to native point defects and unintentional impurities. Oxygen vacancies, zinc interstitials, and hydrogen-related defects are among the most commonly cited contributors, and their presence measurably affects both electrical transport and optical response in ZnO-based devices (Ayoub et al., 2022). A visible green emission band, frequently observed in ZnO photoluminescence spectra, is likewise associated with deep-level defects, particularly vacancies of oxygen and zinc (Ayoub et al., 2022).

Optically, ZnO has a refractive index in the range of 2.0–2.05, a relatively modest value that aids light extraction and supports performance in photonic applications (Vyas, 2020). Taken together, the structural robustness, chemical amphotericity, surface reactivity, wide bandgap, and favorable optical characteristics of ZnO continue to position it as one of the most actively investigated functional materials in nanotechnology and advanced materials science (Borysiewicz, 2019; Sayeem et al., 2026).

Chapter:3 carrot seed

I.4. Botanical Description of Carrot Seeds (*Daucus carota L.*)

I.4.1 Name

Carrot belongs to the genus *Daucus*, family Apiaceae (formerly Umbelliferae), and is scientifically designated as *Daucus carota L.* The species comprises 13 recognized subspecies, of which only one D. carota subsp. sativus (Hoffm.) Arcang. is cultivated for agricultural and commercial purposes, while the remaining subspecies are wild forms (Ismail et al., 2024). The plant is commonly known as carrot in English, carotte in French, and zahra (جزرة) in Arabic. Wild forms are also referred to as "Queen Anne's lace" or "bird's nest" in English-speaking regions (CABI, 2022).

I.4.2 Origin and Geographical Distribution

The carrot is a diploid and biennial vegetable from the Apiaceae family, widely considered to have originated from Afghanistan, and is nowadays cultivated in nearly every country in the world (Koley et al., 2022). Although cultivated for over 2,000 years, and originally used primarily as a medicinal plant, the domestic carrot remains an important world crop, with production expanding rapidly in Asia. Cultivated carrots are mainly classified into eastern and western groups based on root pigmentation; eastern carrots are thought to originate from Afghanistan, while the precise origin of western carrots remains uncertain (Simon et al., 2023).

The species is native to Europe, northern Africa, and southwestern Asia, and has been widely introduced elsewhere in temperate regions, including China, Japan, Australasia, and North America (CABI, 2022). Today, carrot is one of the most economically important root vegetables globally, with world production exceeding 20 million metric tons, consumed raw in salads, cooked in various dishes, and processed into baby foods and other products (Kew Science, 2023).

I.4.3 Pharmacological Activity

Carrot seeds have attracted considerable scientific interest owing to their rich phytochemical content and broad spectrum of biological activities. *Daucus carota L.* has traditionally been recognized for its antilithic, diuretic, carminative, antiseptic, and anti-inflammatory properties, and has been employed in the treatment of urinary calculus, cystitis, gout, prostatitis, and cancer (Ismail et al., 2024).

Phytochemical analysis has revealed remarkable chemical complexity within the seeds. Studies analyzing wild *Daucus carota* subspecies have identified over 310 compounds, including terpenoids, phenylpropenoids, flavonoids, and phenolic acids (Ismail et al., 2024). The seeds are also notable for their essential oil content, which is characterized by high proportions of monoterpenoids and sesquiterpenoids, with carotol, α-pinene, myrcene, limonene, and sabinene among the major constituents (Stanojević et al., 2023).From a pharmacological standpoint, *Daucus carota* has been documented for antioxidant, analgesic, anti-inflammatory, antimicrobial, antifungal, diuretic, gastroprotective, hepatoprotective, anticancer, cardioprotective, and wound-healing activities. However, due to its emmenagogic and abortifacient properties, its use should be avoided during pregnancy (Sahib et al., 2022). Existing in vitro and in vivo studies support the traditional uses of *Daucus carota* in treating infections, inflammation, and cancer, though well-designed preclinical and clinical trials are still necessary to fully establish the safety and efficacy of wild carrot preparations for human use (Ismail et al., 2024).

Chapter 04:

Formulation of a sunscreen

Formulation of a sunscreen

.5.1. Semi-solid preparation(emulsion):

Skin, as the body's outermost protective barrier, is continuously exposed to ultraviolet radiation capable of inducing oxidative damage, chronic inflammation, and long-term mutagenic injury. Sunscreen emulsions are designed to counteract these effects by delivering UV-absorbing or UV-reflecting agents within a vehicle that spreads uniformly across the skin surface (Bhattacharya & Sherje, 2020). Beyond their protective function, the formulation vehicle itself plays a decisive role in determining the overall performance of the sunscreen, since processing conditions, ingredient selection, and emulsification methods all influence droplet dispersion, product appearance, viscosity, and ultimately the photoprotective efficacy of the final preparation (Santos et al., 2025).

I.5.2 Types of Emulsions

I.5.2.1 Definition

An emulsion is a thermodynamically unstable colloidal dispersion consisting of at least two immiscible liquid phases, in which one phase is dispersed as fine droplets within the other. In pharmaceutical and cosmetic science, emulsions are broadly categorized based on the nature of the dispersed and continuous phases (Bipinchandra et al., 2025).

I.5.2.2 Simple Emulsions

Simple emulsions exist in two principal forms. Oil-in-water (O/W) emulsions consist of oil droplets dispersed in an aqueous continuous phase; these tend to be lighter in texture and are preferred for daily-use sunscreens owing to their non-greasy feel and ease of spreadability. Water-in-oil (W/O) emulsions, by contrast, contain water droplets dispersed within an oil continuous phase, offering superior water resistance and occlusive properties better suited to prolonged outdoor exposure (Bipinchandra et al., 2025; Carniel et al., 2025).

I.5.2.3 Multiple Emulsions

Multiple emulsions represent considerably more complex architectures, most notably the water-in-oil-in-water (W/O/W) type, in which small water droplets are first encapsulated within oil droplets, which are then dispersed in an outer aqueous phase. These systems have attracted growing interest in advanced sunscreen development due to their capacity to encapsulate both hydrophilic and lipophilic active ingredients simultaneously, thereby broadening the photoprotective spectrum of the formulation (Bipinchandra et al., 2025).

I.5.3 Emulsifiers

a. Definition

Emulsifiers are amphiphilic surface-active molecules that position themselves at the oil-water interface, reducing interfacial tension and forming a protective stabilizing film around dispersed droplets. Their presence transforms what would otherwise be a rapidly separating two-phase system into a kinetically stable colloidal dispersion (Wang et al., 2023).

b. Role of the Emulsifier

The emulsifier fulfills several simultaneous functions within a sunscreen formulation. It reduces interfacial tension between the oil and water phases, promotes uniform droplet formation during emulsification, and provides mechanical or electrostatic resistance against droplet coalescence over time. Importantly, the type of emulsifier used significantly influences the distribution of UV filter molecules throughout the formulation, which has a direct and measurable impact on the sun protection factor (SPF) of the final product. Experimental evidence has shown that substituting one emulsifier for another for instance, replacing Polysorbate80 with Beautyderm K10produces statistically significant differences in SPF values, rheological behavior, and textural properties, underscoring how critical emulsifier selection is in sunscreen design (Špaglová et al., 2025; Santos et al., 2025).

c. Classification According to HLB Balance

Emulsifiers are systematically classified using the Hydrophilic-Lipophilic Balance (HLB) value, a numerical scale ranging from 0 to 20 that quantifies the relative affinity of an emulsifier molecule for water versus oil. Emulsifiers with low HLB values (approximately 3–6) favor water-in-oil emulsions, whereas those with higher values (approximately 8–18) are more suitable for oil-in-water systems. Crucially, emulsion stability is maximized when the HLB of the emulsifier system closely matches the required HLB of the oil phase; under these matched conditions, optimal stability, smallest droplet size, and the lowest interfacial tension are simultaneously achieved (Wang et al., 2023). The concentration of the emulsifier system also matters: in formulations containing Beautyderm, increasing booster concentration was found to exert the most pronounced effects on textural properties, further illustrating the interdependence between emulsifier choice, concentration, and formulation performance (Špaglová et al., 2025).

I.5.4 Formulation of an Emulsion

The preparation of a sunscreen emulsion follows sequential steps designed to achieve uniform ingredient dispersion and lasting physical stability. Typically, oil-soluble components — including lipophilic UV filters, emollients, and lipophilic emulsifiers — are combined and heated to form the oil phase, while hydrophilic ingredients such as humectants, water-soluble actives, and the aqueous phase are prepared separately before the two phases are united under controlled temperature and agitation (Bipinchandra et al., 2025).

The emulsification method selected has a measurable impact on the properties of the final product. High-shear processing at 15,000 rpm for 15 minutes has been shown to yield emulsions with significantly elevated in vitro SPF values — reaching an average of 42 compared to 30 for conventionally stirred preparations — alongside improved droplet size uniformity (Santos et al., 2025). The concentrations of structural ingredients such as self-emulsifiers, co-emulsifiers, and gelling agents also exert considerable influence on apparent viscosity and the physical stability index of the final sunscreen, a relationship best explored through systematic Quality by Design (QbD) approaches (Carniel et al., 2025).

I.5.5 Quality Control of Emulsions

Quality control of sunscreen emulsions encompasses a comprehensive battery of physicochemical and performance evaluations. Standard assessments include measurement of pH, viscosity, droplet particle size distribution, and zeta potential — the last of these serving as a key indicator of electrostatic colloidal stability. Stability testing under accelerated conditions, centrifugation stress, and freeze-thaw cycling provides evidence of formulation robustness under real-world storage scenarios (Bhattacharya & Sherje, 2020; Carniel et al., 2025). Rheological characterization and texture analysis contribute additional layers of understanding regarding product consistency and sensory performance, with centrifuge testing capable of revealing phase separation tendencies that might not be apparent under ambient storage alone (Špaglová et al., 2025). In vitro SPF determination and photostability evaluation under UV irradiation represent the primary performance benchmarks guiding both formulation optimization and regulatory submission (Santos et al., 2025).

Part 2

Practical work

Chapter05 Material and method

II.1. Plant Material:

The selection of carrot seeds (*Daucus carota L.*) was based on their richness in various bioactive compounds, making them a promising plant source for green synthesis and contributing to the development of safe and environmentally friendly pharmaceutical and cosmetic applications. The plant was identified and validated by Dr. Hacene LAOUDJE, from the Department of Biology at the University of El Oued.

Figure 10. Carrot seeds (*Daucus carota L.*) used in the present study **(Original photo, 2026).**

A. Chemicals:

Zinc acetate (Zn $(OOCCH_3)_2 \cdot 2H_2O$),
Methanol
Folin -Ciocalteu reagent
Aluminum chloride($AlCl_3$)
Quercetin (standard)
gallic acid(standard)
Distilled water
DPPH (2,2-diphenyl-1-picrylhydrazyl)

B. Apparatus:

Electronic mill
Magnetic stirrer
Filter paper
Centrifuge
Thermometer
Electronic balance
UV–Visible spectrophotometer
Analytical balance
Micropipettes
Vortex mixer
Water bath
Volumetric flasks and test tubes

C. Glassware

Glass test tubes
Pipette
Beaker
Erlenmeyer flask
Graduated cylinder
, Sink
Funnel
Spatula
Watch glass
Wash bottle
Syringe
Mortar and pestle

II.2. Biological Material:

II.2.1. Bacterial Strains

The bacterial strains used in this study were obtained from El Majd Laboratory, El Oued, Algeria. The strains were sub cultured on nutrient agar and maintained at 4°C until further use. Three bacterial species were selected to evaluate the antibacterial activity of the synthesized nanoparticles. Their Gram characteristics and associated pathogenicity are presented in Table 3.

Table 2: Characteristics of the bacterial strains used in this study

Strain	**Staphylococcus aureus**	**Escherichia coli**	**Pseudomonas aeruginosa**
Gram	Gram+	Gram-	Gram -
Pathogenic potential	Skin infections (furuncles, abscesses), wound infections, respiratory tract infections.	Urinary tract infection, gastrointestinal infections, septicemia.	Wound infections, respiratory infection, urinary tract infections nosocomial infections.

II.2.2 Biosynthesis of nanoparticules:

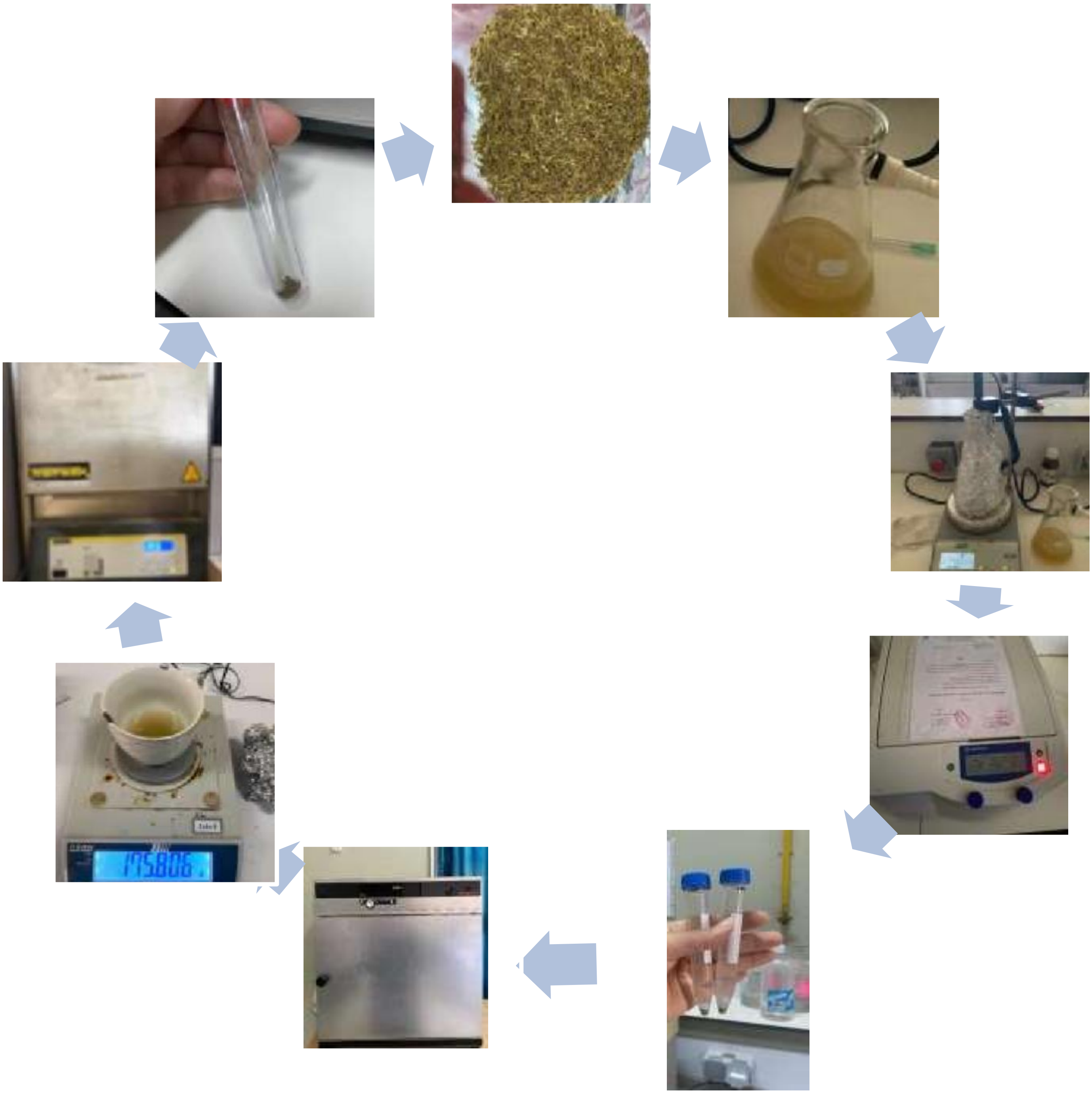

Figure11. Schematic representation of the green synthesis procedure of ZnO nanoparticles using *Daucus carota* seed extract **(Original photos, 2026**).

II.2.2.1. Preparation of Carrot Seed :

Carrot seeds (*Daucus carota L.*) were cleaned manually to remove impurities and foreign materials. The seeds were washed thoroughly with distilled water and allowed to dry at room temperature. After complete drying, the seeds were ground using an electric grinder to obtain a fine powder. The powder was stored in a clean, dry, airtight container until further use Biosynthesis of Zinc Oxide Nanoparticles (ZnO-NPs)

II.2.2.2. Preparation of Carrot Seed Extract

- *Daucus carota L.* seeds were cleaned, washed with distilled water, dried, and ground into a fine powder.
- A quantity of 2.5 g of seed powder was mixed with 250 mL of distilled water.
- The mixture was heated under continuous stirring to facilitate the extraction of bioactive compounds.
- After extraction, the solution was filtered to remove solid residues and obtain a clear aqueous extract.

II.2.2.3. Green Synthesis of Zinc Oxide Nanoparticles

- 10.43 g of zinc acetate dihydrate [$Zn(CH_3COO)_2 \cdot 2H_2O$] was dissolved in 350 mL of distilled water.
- The solution was heated at 70–80°C under continuous magnetic stirring.
- 210 mL of carrot seed extract aqueous was added dropwise to the zinc acetate solution while maintaining constant stirring.
- The reaction mixture was kept under stirring at the same temperature for 2 hours to ensure complete reaction and nanoparticle formation.
- Phytochemicals present in the extract acted as reducing and stabilizing agents, promoting the formation and stabilization of ZnO nanoparticles.

a. Purification of Nanoparticles

- The resulting colloidal suspension was kept in the dark at room temperature for 24 hours.
- The mixture was centrifuged for 40 minutes.
- The supernatant was discarded, and the pellet was resuspended in an equal volume of distilled water.
- A second centrifugation was carried out for 30 minutes.
- The washing process was repeated three times to remove residual impurities and unreacted compounds.

b. Drying and Calcination

- The purified pellet was dried in an incubator at 70°C until complete dryness.
- The dried powder was then subjected to calcination at 600°C for 5 hours.
- Calcination removed residual organic matter and converted the intermediate compounds into highly crystalline zinc oxide.
- Finally, a white powder of zinc oxide nanoparticles (ZnO-NPs) was obtained and stored in airtight containers for further characterization and biological evaluation.

c. characteristic of nanoparticules:

Our analysis was performed using Fourier transform infrared (FT-IR) spectroscopy at the laboratory of the Faculty of Natural and Life Sciences. The study of the structure of materials at the nanoscale, particularly semiconductors, relies on a set of advanced techniques. Among the most common are X-ray diffraction (XRD) and Fourier transform infrared (FT-IR) spectroscopy. These valuable analytical tools allow us to characterize and understand in detail the structural properties of these nanomaterials.

- **XRD (X ray diffraction)**

It should be noted that the X-ray diffraction analysis was carried out at the Materials Analysis Laboratory of the Faculty of Exact Sciences. The obtained nanoparticle powders were placed on a glass slide and then analyzed using X-ray diffraction (XRD). This analysis was performed using an Expert Pro Panalytical X-ray diffractometer, employing Cu Kα radiation, with scanning in the range of 25° to 70°, an angular step of 0.25°, a counting time of 16 s, a generator voltage of 45 kV, and a tube current of 40 mA (Ghellab et al., 2023).

Figure12: the X-ray diffraction **(Original photo, 2026)**

- **UV–Visible Spectroscopy**.

10 mg of ZnO NP powder was weighed and transferred to a 10 mL volumetric flask of water. The solution was then placed in an ultrasonic bath for 40 minutes at a power of 60 watts and a temperature of 35 °C. The spectrum of zinc oxide nanoparticles was determined in the UV/V range from 800 to 290 nm. (Ghellab et al., 2023).

Figure13: Spectrophotometer SHIMADZU UV-1201 **(Original photo, 2026)**

- **Fourier Transform Infrared Spectroscopy (FTIR):**

Fourier transform infrared (FTIR) spectroscopy was carried out using a BSAC WQF-530A FTIR spectrometer (Beijing Beifen-Ruili Analytical Instrument Co) equipped with an attenuated total reflectance (ATR) accessory . The instrument operates over a spectral range of 350–7800 cm^{-1}, with a signal-to-noise ratio of 20,000:1 and a resolution of 0.85 cm^{-1}(Malaiappan et al., 2024). The powder samples were placed directly onto the ATR crystal without prior preparation, and spectra were acquired in the wavenumber range of 400–4000 cm^{-1} to identify the characteristic absorption bands corresponding to the Zn–O stretching vibration as well as residual organic functional groups derived from the *Daucus carota* seed extract.

II.2.2.4. Study of antimicrobial effect:

II.2.2.4.1. Preparation of Culture Medium

Mueller–Hinton agar (MHA) was selected as the reference culture medium for antimicrobial susceptibility testing, in accordance with standard microbiological guidelines. The medium was prepared by dissolving the appropriate quantity of dehydrated MHA powder in distilled water according to the manufacturer's instructions. The solution was then sterilized by autoclaving at 121°C for 15 minutes. After sterilization, the medium was allowed to cool to approximately 45–50°C under aseptic conditions before being poured into sterile Petri dishes. Plates were left to solidify at room temperature and subsequently stored at 4°C until use (Joffin & Leyral, 2003).

II.2.2.4.2. Preparation of Inoculum

Three reference bacterial strains were employed in this study: *Escherichia coli* ATCC 25922 and *Pseudomonas aeruginosa* ATCC 27853, both Gram-negative organisms, and *Staphylococcus aureus* ATCC 25932, a Gram-positive representative. For each strain, an inoculum was generated from the stock culture on Mueller–Hinton broth and incubated at 37°C for 24 hours. Following incubation, the bacterial suspensions were adjusted to a turbidity equivalent to the 0.5 McFarland standard (approximately 1 × 106 CFU mL-1) using sterile physiological saline solution (0.9% NaCl). The standardized inocula were prepared under aseptic conditions within 15 minutes prior to use (Bonev et al., 2008).

II.2.2.4.3. Preparation of Carrot Seed Extract and Zinc Oxide Nanoparticles

For Testing Two test samples were prepared and evaluated in this study: Sample R — Green-synthesized zinc oxide nanoparticles (ZnO-NPs) obtained using the methanolic extract of *Daucus carota L.* seeds as a bioreducing agent. This sample was dissolved in 5% dimethyl sulfoxide (DMSO) to ensure adequate solubility prior to testing. Sample R' — Raw methanolic extract of *Daucus carota L.* seeds, also dissolved in 5% DMSO and used as a comparative reference to evaluate the contribution of plant phytochemicals alone. Both samples were tested at four working concentrations: 10, 7.5, 5, and 2.5 mg mL-1. All solutions were freshly prepared under aseptic conditions immediately before testing to preserve their biological activity.

II.2.2.4.4. Seeding the standardized bacterial suspensions

Were uniformly spread over the entire surface of Mueller–Hinton agar plates using sterile cotton swabs, with three sequential passes in different directions to ensure a homogeneous confluent bacterial lawn. The inoculated plates were then left to dry under aseptic conditions near a Bunsen burner for approximately 15 minutes before well preparation, allowing the bacterial suspension to be fully absorbed into the agar surface (Joffin & Leyral, 2003).

II.2.2.4.5. Agar-Well Diffusion Method

The agar-well diffusion method was employed to evaluate the antibacterial activity of both test samples. Using sterile cork borers, uniform wells of 6 mm diameter were created in the seeded

Figure14. Main steps of the agar well diffusion assay used for antibacterial activity evaluation **(Original photo, 2026)**

MHA plates. Each well was loaded with 50 µL of the corresponding test solution at each of the four concentrations tested (10, 7.5, 5, and 2.5 mg mL-1). Appropriate controls were included in all experiments: wells containing 5% DMSO served as negative controls, while gentamicin (10 µg/disc equivalent concentration) was used as the positive control to confirm bacterial susceptibility and assay validity.

The inoculated plates were subsequently incubated at 37°C for 24 hours under aerobic conditions. After incubation, the diameters of the inhibition zones (mm) surrounding each well were measured using a calibrated digital caliper, with the 6 mm well diameter included in all measurements. An inhibition zone diameter greater than 6 mm was considered indicative of antibacterial activity (Bonev et al., 2008; Kiehlbauch et al., 2000)

II.2.2.5. Study of the Antioxidant Effect

II.2.2.5.1. Principle of the DPPH Radical Scavenging Assay

The antioxidant activity of both test samples was evaluated using the 2,2-diphenyl-1-picrylhydrazyl (DPPH) free radical scavenging assay, one of the most widely applied and reliable in vitro methods for assessing the antioxidant potential of plant-derived materials and nanomaterials (Soare et al., 1997; Sreelatha & Inbavalli, 2012).

DPPH is a stable free radical that exhibits a characteristic deep purple color in solution. In the presence of an antioxidant compound capable of donating a hydrogen atom or an electron, the DPPH radical is reduced to its non-radical form DPPH-H, which is yellow in color. This color change is accompanied by a measurable decrease in absorbance at 517 nm, and the extent of this decrease is directly proportional to the radical scavenging capacity of the tested sample (Dziri et al., 2012).

II.2.2.5.2. Preparation of the DPPH Solution

A stock solution of DPPH was prepared by dissolving the appropriate quantity of DPPH powder in methanol to obtain a working concentration of 0.25 mm The solution was freshly prepared on the day of each experiment, protected from light, and stored at 4°C until use to prevent radical degradation (Benhammou et al., 2009).

II.2.2.5.3. Preparation of Sample Solutions

Two test samples were evaluated independently using the same protocol:

• Sample R — Green-synthesized ZnO nanoparticles (*Daucus carota L.* seed extract + zinc acetate), dissolved in methanol.

• Sample R' — Raw methanolic extract of *Daucus carota L.* seeds, dissolved in methanol.

• Positive control — Ascorbic acid (Vitamin C), prepared in methanol at the same concentration range as the test samples. Each sample was prepared at nine working concentrations: 0.01, 0.05, 0.1, 0.15, 0.2, 0.25, 0.3, 0.35, and 0.4 mg mL-1, by serial dilution from a stock solution, in accordance with the method described by Benhammou et al. (2009).

II.2.2.5.4. Experimental Procedure For each concentration tested

500 µL of the sample solution was mixed with 500 µL of the 0.25 mm DPPH methanolic solution in a test tube. The mixture was vortexed briefly and then incubated at room temperature in the dark for 30 minutes to allow the radical scavenging reaction to reach completion. A blank was prepared by replacing the sample with an equal volume of pure methanol, while the negative control consisted of DPPH solution mixed with methanol only (without any sample). All experiments were performed in triplicate (Benhammou et al., 2009).

II.2.2.5.5. Absorbance Measurement and Calculation

After the 30-minute incubation period, the absorbance of each reaction mixture was measured at 517 nm using a UV-Visible spectrophotometer (SHIMADZU UV-1201). The percentage of DPPH radical scavenging inhibition (I%) for each concentration was calculated according to the following equation:

$I(\%) = ((A0 - Ai) / A0) \times 100$ • A0 : Absorbance of the control (DPPH + methanol, without sample)

• Ai : Absorbance of the test sample at each concentration

II.2.2. 5.6. Determination of IC_{50}

The antioxidant potency of each sample was quantified by determining its IC50 value, defined as the concentration of sample required to inhibit 50% of the DPPH free radical activity. The IC50 was calculated by plotting the inhibition percentage (I%) against the corresponding sample concentration and interpolating the concentration corresponding to 50% inhibition from the resulting dose–response curve (Dziri et al., 2012). A lower IC50 value indicates higher antioxidant activity. The IC50 values of both samples (R and R') were compared to that of ascorbic acid (Vitamin C) used as a positive reference standard.

Figure 15**.** DPPH assay procedure **(Original photo, 2026)**.

II.2.2.6. Study of the Photoprotective Effect

II.2.2.6.1. Determination of Sun Protection Factor (SPF)

The photoprotective activity of both test samples was assessed through the in vitro determination of the Sun Protection Factor (SPF). This method evaluates the ability of a substance to reduce ultraviolet irradiation by measuring the transmittance of radiation through a film of the product. When operative conditions of transmission measurement are properly controlled, this approach yields precise and reproducible values, expressed as a single UV absorbance curve (Miloudi et al., 2025).

II.2.2.6.2. Measurement of pH

The pH of both test samples was measured using a calibrated digital pH meter. Measurements were carried out after a defined storage period to assess the physicochemical stability of the preparations under different storage conditions. An ideal pH value for skin-applied formulations is approximately 6.0, which is close to the natural pH of human skin. Variations in pH over time may reflect the occurrence of chemical reactions within the formulation and can serve as a reliable indicator of its overall quality and stability (Kerri et al., 2019).

Figure16 : Ph meter **(Original photo, 2026)**

II.2.2.7. Formulation of Sunscreen Based on Carrot Seed Extract and Zinc Oxide Nanoparticles

II.2.2.7.1. Composition of Sunscreen

The sunscreen formulation developed in this study consisted of the following ingredients: Lanette O (5 g) as the emulsifying wax, Emulgin (4 g) as a non-ionic co-emulsifier, almond oil (10 g) as the oily phase, distilled water (57 g) as the aqueous phase, vitamin E as an antioxidant stabilizer, and green-synthesized zinc oxide nanoparticles (ZnO-NPs) (20 mg) as the active UV-filtering agent. The combination of these excipients was selected to produce a stable oil-in-water (O/W) emulsion suitable for topical skin application (Kerri et al., 2019).

II.2.2.7.2. Preparation of Cream

The cream was prepared following a standard hot emulsification method. Lanette O, Emulgin, and almond oil were accurately weighed and combined in a beaker, then heated together in a water bath at approximately 70°C until a clear and homogeneous oil phase was obtained. Simultaneously, distilled water was heated to the same temperature in a separate beaker to prepare the aqueous phase.

The ZnO-NPs (20 mg) were first dispersed in a small portion of the oil phase and thoroughly mixed to ensure their uniform distribution throughout the formulation. The aqueous phase was then added slowly and dropwise to the oil phase under continuous stirring and mechanical homogenization until a stable and uniform emulsion was formed.

Figure 17. Cream formulation process**(Original photo, 2026)**.

The emulsion was maintained under continuous stirring throughout the cooling process. When the temperature reached approximately 40–45°C, vitamin E was incorporated into the mixture. Stirring was continued until the cream cooled to room temperature and achieved a smooth, homogeneous, and stable consistency. The final product was transferred into clean, airtight containers and stored under appropriate conditions for further analysis (Arias et al., 2022).

II.2.2.7.3. Quality Control Analysis of Cream

The quality of the prepared sunscreen cream was evaluated through two physicochemical parameters: the Sun Protection Factor (SPF) and pH measurement. The SPF was determined in vitro by measuring the absorbance of the cream dissolved in ethanol at 1 mg/mL across seven wavelengths from 290 to 320 nm at intervals of 5 nm, using a UV-Visible spectrophotometer, and calculated according to the Mansur et al. (1986) equation: $SPF = CF \times \Sigma (EE(\lambda) \times I(\lambda) \times DO(\lambda))$. The pH was measured using a calibrated digital pH meter after a defined storage period, with an ideal target value of approximately 6.0, close to the natural pH of human skin (Kerri et al., 2019; Miloudi et al., 2025; Osterwalder & Herzog, 2009).

Chapter 06: Results and Discussion

III.1. Extraction Yield of *Daucus carota L.* Seed Extract

The extraction yield of *Daucus carota L.* seeds was calculated according to the following formula (Miloudi et al., 2025):

Yield (%) = (Weight of extract / Weight of dry plant material) × 100

The results obtained are summarized in Table 5 below.

Table 3: Extraction yield of *Daucus carota L.* seed methanolic extract.

Parameter	Value
Weight of dry plant material (g)	2
Weight of crud extract (g)	0.1997
Extraction yiled (%)	9.99

III.2. Phytochemical Characterization of Carrot Seed Extract

III.2.1 Phenolic Content

The calibration curve constructed for total phenolic content determination showed a positive linear relationship between gallic acid standard concentrations and the measured absorbance values, expressed by the regression equation y = 0.0053x +0.0128, with a coefficient of determination R^2 = 0.9421 (Figure11).

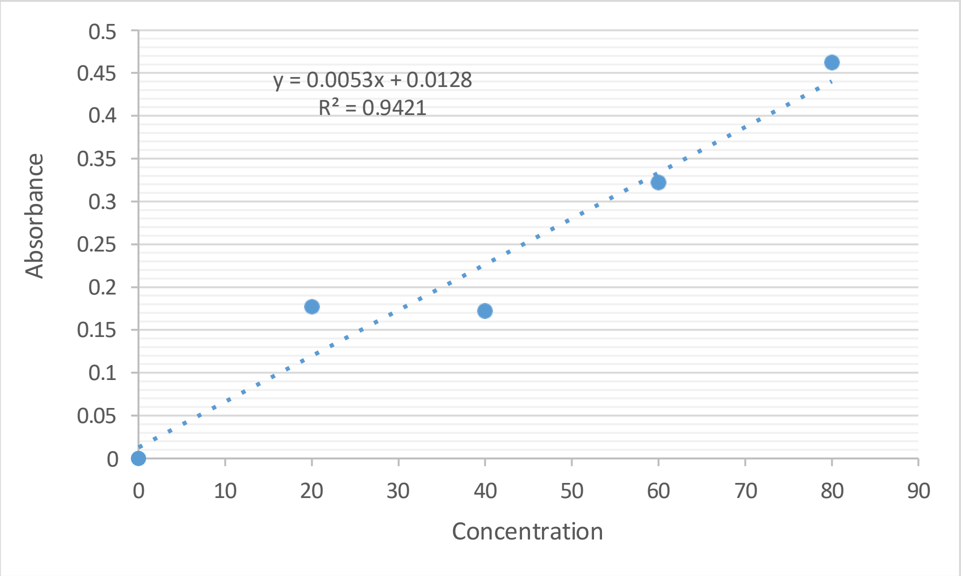

Figure18: The Calibration Model For Phenolic

The consistent increase in absorbance with rising concentrations confirms the proportional response of the Folin–Ciocalteu method within the tested range, and the high R^2 value reflects good linearity and limited experimental deviation, validating the reliability of the calibration model for phenolic quantification (Ersoy et al., 2024).

The satisfactory linearity can be attributed to the efficient interaction between phenolic compounds and the Folin–Ciocalteu reagent, which produces a stable blue chromophore whose intensity increases proportionally with concentration. These results are consistent with those reported in comparable spectrophotometric studies of plant-derived extracts, where similar linear correlations were observed for total phenolic content determination, further confirming the accuracy and reproducibility of the analytical procedure adopted in the present work (Ersoy et al., 2024).

III.2.2. Flavonoid

The calibration curve established for flavonoid quantification revealed a positive linear relationship between quercetin standard concentrations and the corresponding absorbance values, described by the regression equation $y = 0.0143x + 1.281$, with a coefficient of determination $R^2 = 0.9397$ (Figure11).

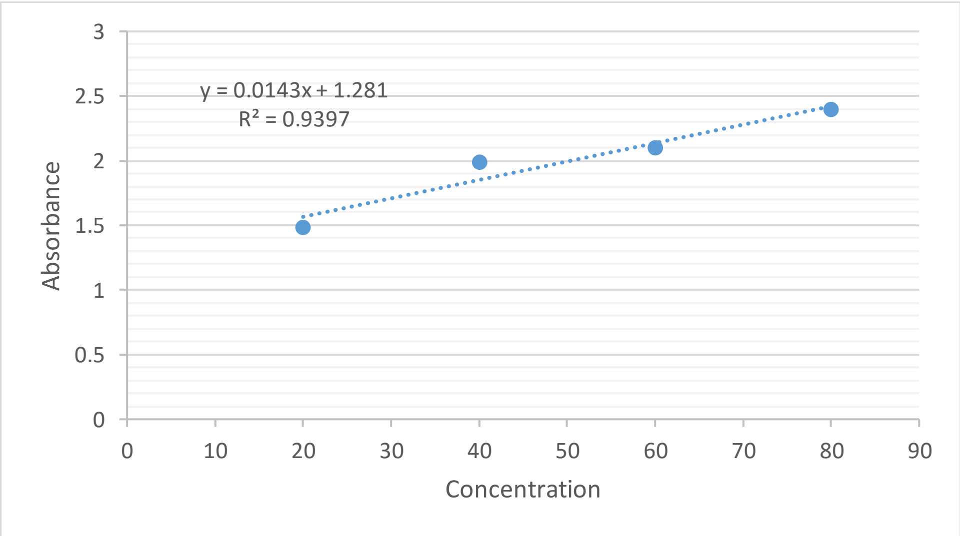

Figure 19: The Calibration Curve established for Flavonoid

The progressive increase in absorbance with rising concentrations confirms the proportional response of the method within the studied range, while the satisfactory R^2 value reflects an acceptable degree of linearity, supporting the suitability of this calibration model for quantitative flavonoid determination (Chutulo et al., 2020).

The efficient formation of the flavonoid–reagent complex resulted in stable and concentration-dependent color development, which minimizes potential analytical errors in the subsequent calculation of total flavonoid content. These results are in agreement with previously reported spectrophotometric analyses of plant extracts, where similar linear relationships were established between standard concentrations and absorbance values for flavonoid quantification, confirming the reliability of this approach as an analytical tool for phytochemical characterization (Chutulo et al., 2020).

III.2.3. Tannin Content

The calibration curve constructed for tannin quantification demonstrated a strong positive linear relationship between tannic acid standard concentrations and the corresponding absorbance values, expressed by the regression equation $y = 0.02x - 0.0015$, with a coefficient of determination $R^2 = 0.9826$ (Figure20).

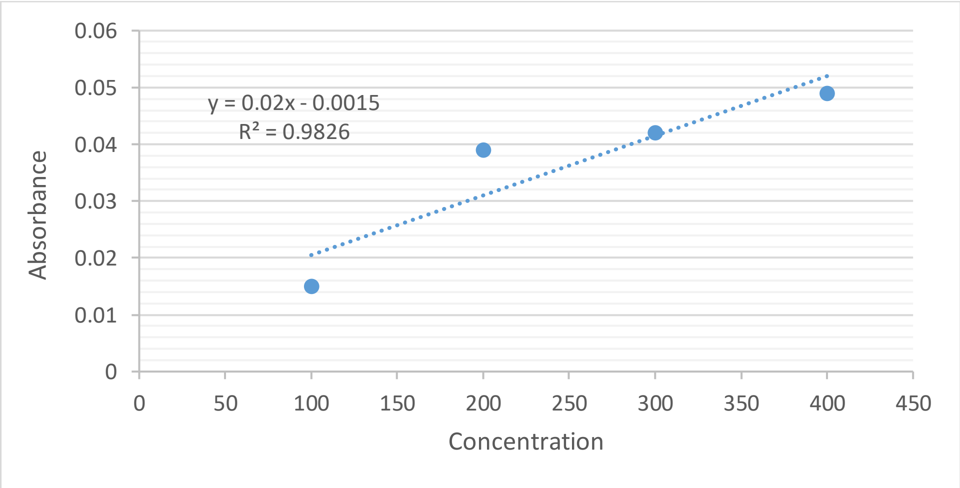

Figure 20: The Calibration Curve Constructed For Tannin.

This high R^2 value reflects excellent linearity across the studied concentration range, confirming both the sensitivity and the reliability of the calibration model for tannin determination. The steady increase in absorbance with rising concentrations further validates the proportional response of the analytical method (Mughal et al., 2018).

The excellent linearity recorded can be attributed to the efficient interaction between tannin compounds and the analytical reagent, generating a stable colored complex whose absorbance responds proportionally to concentration changes. The minimal experimental deviation indicated by the high coefficient of determination confirms the precision and reproducibility of the procedure. These results are in line with findings reported in comparable spectrophotometric studies of plant extracts, where strong linear correlations were similarly established for tannin quantification, supporting the validity of the analytical approach adopted in the present work (Mughal et al., 2018).

III.2.4. Quantitative Estimation of Phytochemical Constituents

The quantitative phytochemical analysis of *Daucus carota L.* seed extract revealed notable differences in the concentrations of the three investigated classes of bioactive compounds (Figure21).

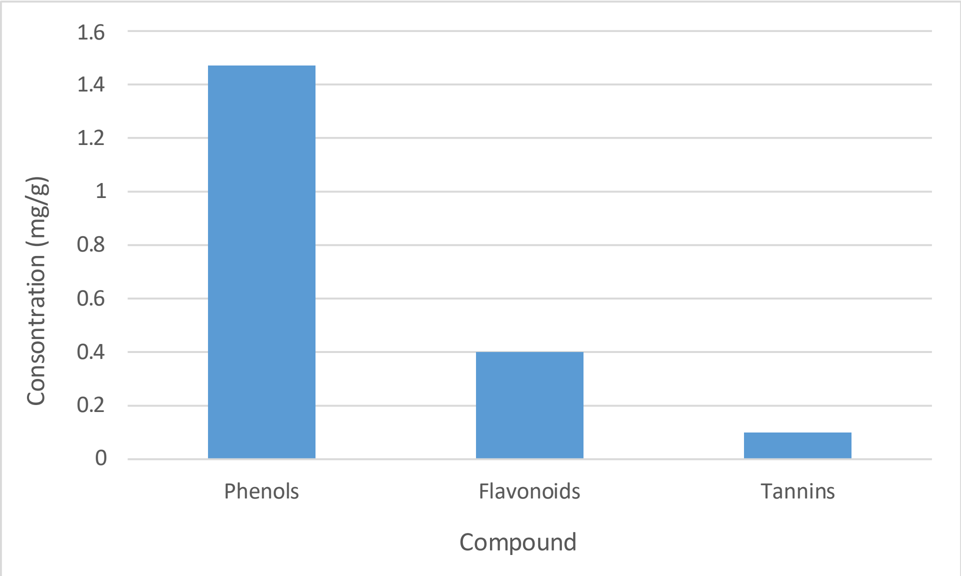

Figure21: Quantitative Estimation of Phytochemical Constituents

Phenolic compounds represented the dominant constituent with an approximate value of 1.5 mg/g of dry matter, followed by flavonoids at approximately 0.4 mg/g of dry matter, while tannins were detected in the lowest amount, estimated at around 0.1 mg/g of dry matter.

The predominance of phenolic compounds over other secondary metabolites is consistent with findings (reported by Nasiruddin & Sinha 2020), who similarly observed that phenolics constituted the major phytochemical class in plant extracts, with flavonoids and tannins present in comparatively lower quantities. This comparable distribution pattern suggests a shared biosynthetic tendency across plant-derived extracts rich in polyphenolic compounds.

The elevated phenolic content recorded in the present study may reflect the strong capacity of *Daucus carota* seeds to synthesize phenolic metabolites as protective molecules against oxidative stress and environmental pressures. Given their well-established ability to donate electrons and hydrogen atoms, phenolic compounds are expected to play a central role in the radical scavenging activity of this extract. The relatively low flavonoid content, on the other hand, may be influenced by factors such as solvent polarity, extraction conditions, plant origin, or seasonal and physiological variation in secondary metabolite accumulation. The moderate tannin content likely contributes to both the antioxidant and antimicrobial properties of the extract through complexation with proteins and metal ions (Nasiruddin & Sinha, 2020).

III.3. The antioxidant activity:

For the DPPH test, the value shown corresponds to the IC_{50}. The value shown corresponds to the comparative value calculated from the regression line، because this test measure absorbance capacity and not direct radical inhibition.

III.3.1. DPPH Free Radical Antioxidant Activity

As shown in Figure 22, the DPPH curve of the extract indicates an increase in the percentage of inhibition with concentration: inhibition increases from 5% at 3.35 µg/mL to 58% at 80 µg/mL. This trend reflects a dose-dependent response of the extract to the DPPH radical. The concentration of the extract (µg/mL) is represented on the x-axis, while the percentage of DPPH radical inhibition (%) is represented on the y-axis. The regression line is as follows: $y = 0.7088x - 0.0944$; $R^2 = 0.8803$; $CI_{50} = 70.67$ µg/mL

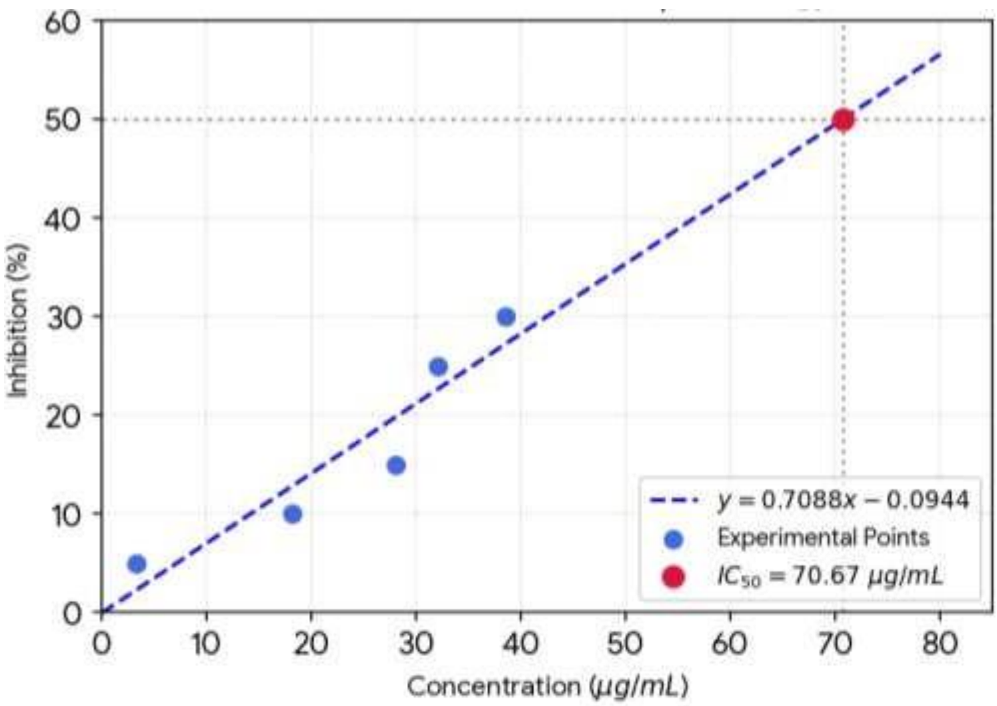

Figure 22: Antioxidant activity of extract as a function of concentration

III.3.2 Ascorbic acid antioxidant activity

The antioxidant activity of ascorbic acid demonstrated a strong positive correlation between concentration and scavenging activity, as evidenced by the progressive increase in response values with increasing concentration. The regression coefficient ($R^2 = 0.988$) indicates excellent linearity and confirms the reliability of the obtained analytical results. This behavior reflects the well-known antioxidant capacity of ascorbic acid, which acts as an effective reducing agent capable of donating electrons or hydrogen atoms to neutralize free radicals.

The obtained results are consistent with those reported by Sing et al., who highlighted the concentration-dependent antioxidant activity of bioactive compounds. This agreement supports the effectiveness of antioxidant molecules in scavenging reactive oxygen species and reducing oxidative stress.

The high antioxidant activity observed may be attributed to the strong reducing power of ascorbic acid and its ability to inhibit oxidation reactions. The gradual increase in activity with concentration confirms the dose-dependent behavior commonly associated with antioxidant standards. Minor deviations from ideal linearity may be related to experimental conditions such as measurement sensitivity, reagent stability, or sample handling. Nevertheless, the high regression coefficient indicates excellent precision and reproducibility.

Overall, the results confirm the strong antioxidant potential of ascorbic acid and validate its suitability as a reference standard for antioxidant evaluation. The regression line is as follows: $y = 3.1851x + 33.118$; $R^2 = 0.988$; $CI_{50} = 5.30$ µg/mL

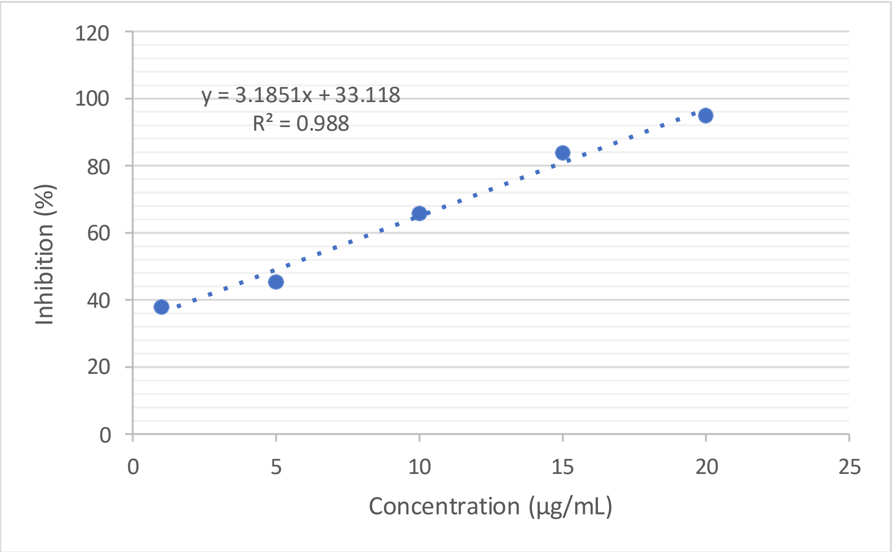

Figure 23: Antioxidant activity of ascorbic acid as a function of concentration

III.4. ZnO nanoparticles antioxidant activity

The antioxidant activity of ZnO nanoparticles exhibited a concentration-dependent increase, as indicated by the progressive elevation in response values with increasing nanoparticle concentration. The regression coefficient ($R^2 = 0.9659$) reflects a strong linear relationship, confirming the reliability and consistency of the obtained results.

The findings are consistent with those (reported by Djafarou et al.,) who demonstrated that ZnO nanoparticles synthesized through eco-friendly approaches exhibited significant antioxidant activity that increased with concentration. This supports the role of ZnO nanoparticles in reducing oxidative stress and scavenging reactive oxygen species.

The antioxidant potential may be attributed to the physicochemical properties of ZnO nanoparticles, including high surface area, nanoscale dimensions, and active surface sites. Surface defects and oxygen vacancies may further enhance electron transfer processes involved in radical scavenging mechanisms. Minor deviations from linearity may be due to nanoparticle aggregation, particle size distribution, or experimental conditions. However, the high correlation coefficient confirms good analytical reliability.

Overall, the results demonstrate that ZnO nanoparticles possess considerable antioxidant activity with potential biomedical and pharmaceutical applications. The regression line is as follows: $y = 2.5162x - 5.7508$; $R^2 = 0.9659$; $CI_{50} = 22.16$ µg/mL

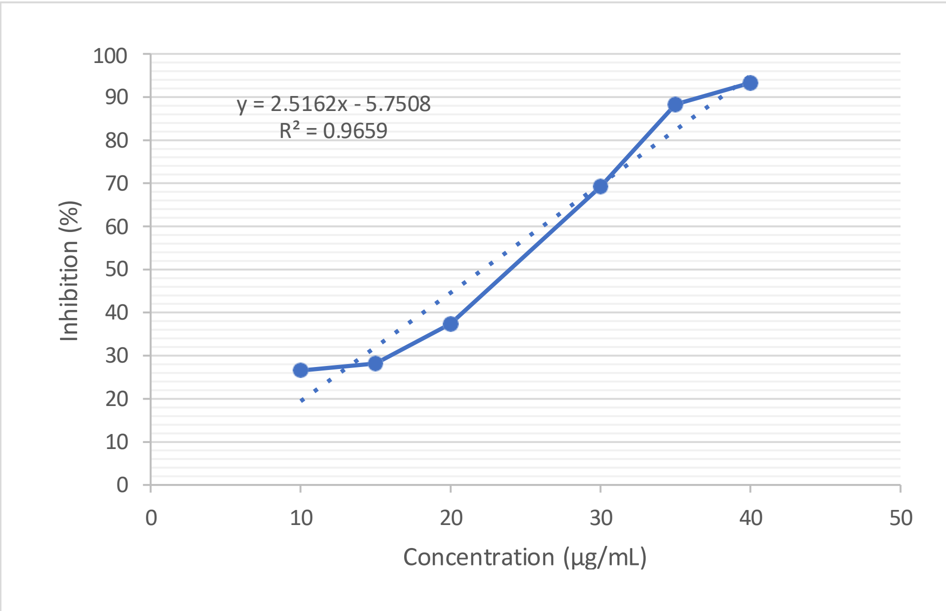

Figure24: Antioxidant activity of synthesized ZnO nanoparticles at different concentrations

III.4.1. Characterization of ZnO Nanoparticles

III.4.1.1. X-Ray Diffraction Analysis

The XRD pattern of the biosynthesized ZnO nanoparticles displayed a series of well-resolved diffraction peaks at approximately 31.8°, 34.4°, 36.2°, 47.5°, 56.6°, 62.8°, 66.4°, 67.9°, 69.1°, 72.6°, and 77.0° (2θ), indexed to the crystallographic planes (100), (002), (101), (102), (110), (103), (200), (112), (201), (004), and (202), respectively (Figure25).

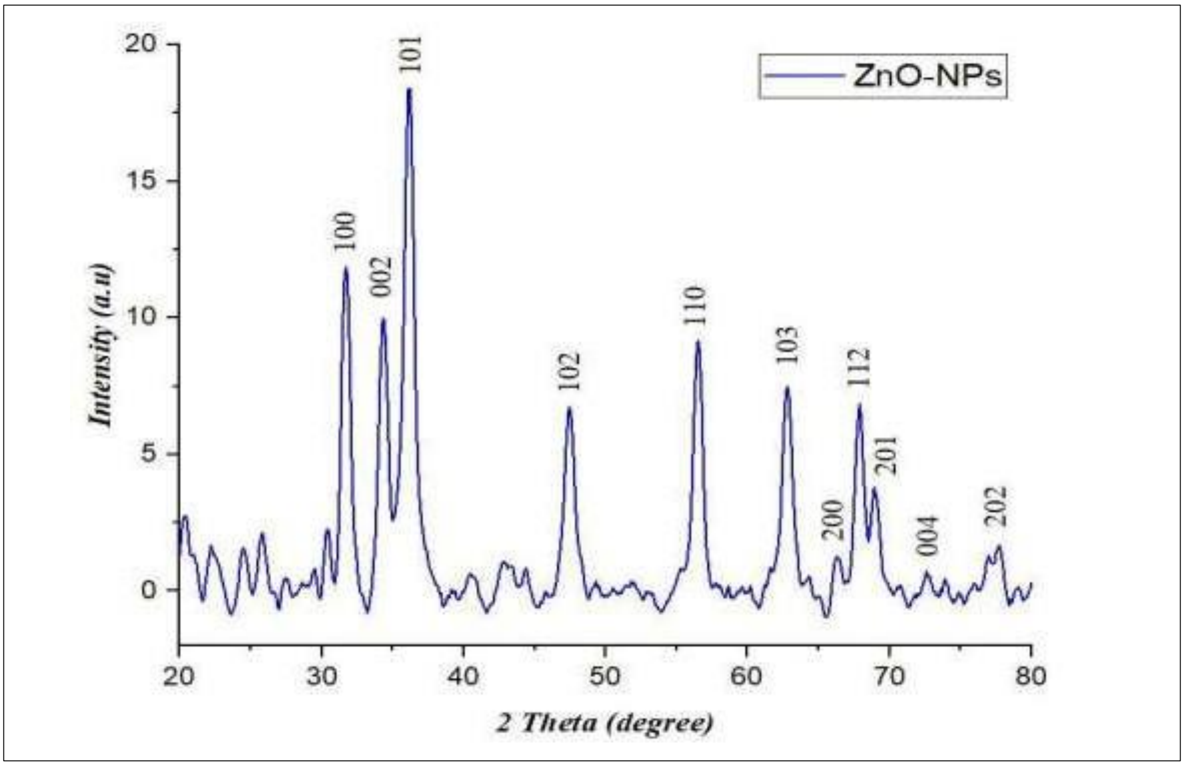

Figure25: X-Ray Diffraction Analysis

The appearance of these characteristic reflections unambiguously confirms the formation of crystalline ZnO nanoparticles with a hexagonal wurtzite structure. The sharpness and high intensity of the diffraction peaks, most notably the dominant (101) reflection, indicate a high degree of crystallinity and well-ordered structural arrangement of the synthesized material (Naqvi et al., 2011; Zidi et al., 2020).

The complete absence of additional peaks attributable to secondary phases or impurity compounds confirms the high purity of the synthesized ZnO-NPs. The pronounced intensity along the (101) plane further suggests preferential crystal growth in this direction, a feature commonly reported for ZnO nanostructures. These results are consistent with those of (Naqvi et al. 2011), who identified identical hexagonal wurtzite diffraction planes in Cr-doped ZnO nanoparticles, and with (Zidi et al. 2020), who confirmed the preservation of the ZnO crystalline structure under varying synthesis and processing conditions. The high crystallinity achieved in the present work may be attributed to the effectiveness of the green synthesis procedure, which promoted the formation of a well-ordered hexagonal lattice through the action of bioactive phytochemicals present in the *Daucus carota* seed extract.

III.4.1.2. Fourier Transform Infrared Spectroscopy (FTIR):

The FTIR spectrum of the synthesized ZnO nanoparticles exhibited several characteristic absorption bands that confirm the successful formation of zinc oxide nanostructures.

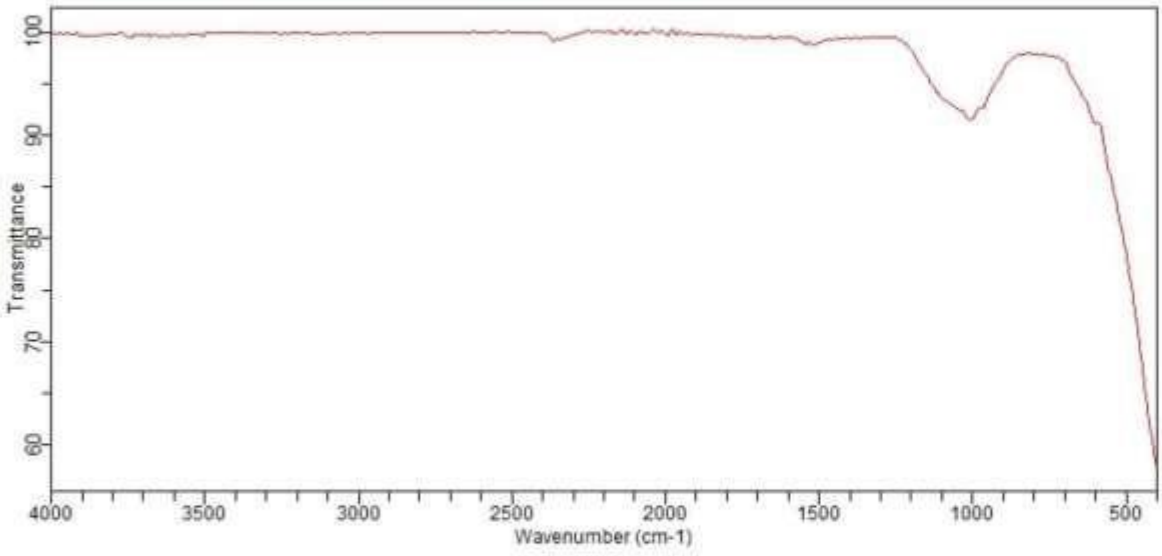

Figur26: FTIR Spectroscopy Analysis

A noticeable absorption band was observed in the region around 1000–1100 cm^{-1}, which may be attributed to C–O stretching vibrations of alcohols, phenolic compounds, or other oxygen-containing functional groups originating from the plant extract used during the synthesis process. These biomolecules are known to act as reducing and stabilizing agents during nanoparticle formation. The most significant feature of the spectrum was the intense absorption band detected below 600 cm^{-1}, particularly in the region of 400–500 cm^{-1}, which is characteristic of Zn–O stretching vibrations and is considered a fingerprint region for zinc oxide nanoparticles. The presence of this band confirms the successful conversion of zinc precursor salts into ZnO nanoparticles. Moreover, the relatively weak absorption bands observed in the higher wavenumber regions indicate that only a limited amount of organic residues remained on the nanoparticle surface after synthesis and purification. These findings suggest that the phytochemicals present in the carrot seed extract participated in the reduction and stabilization processes while allowing the formation of highly purified ZnO nanoparticles.

The obtained results are in agreement with previous studies, including the work reported by the IJCRT study, where characteristic Zn–O stretching vibrations were also observed in the low-frequency region below 600 cm^{-1}. Similarly, the spectral data reported in the NIST database for zinc oxide indicate the presence of absorption bands associated with Zn–O bonds within the same region. The consistency between the present FTIR spectrum and the reference spectra confirms the successful synthesis of ZnO nanoparticles and supports the reliability of the green synthesis approach employing carrot seed extract. The slight differences in peak positions and intensities between the current study and the literature may be attributed to variations in synthesis conditions, particle size, crystallinity, and the nature and concentration of phytochemical compounds adsorbed on the nanoparticle surface.

Overall, the FTIR analysis demonstrates that the synthesized nanoparticles possess the characteristic chemical structure of zinc oxide and confirms the involvement of bioactive compounds from carrot seed extract in nanoparticle formation and stabilization. The presence of Zn–O vibrational bands together with signals corresponding to residual organic functional groups provides strong evidence for the successful green synthesis of ZnO nanoparticles.

III.4.1.3. UV-Visible Spectroscopy Analysis

The UV–Visible absorption spectrum of the biosynthesized ZnO nanoparticles revealed a characteristic absorption peak at approximately 365 nm (Figure 27), confirming the successful formation of ZnO nanostructures.

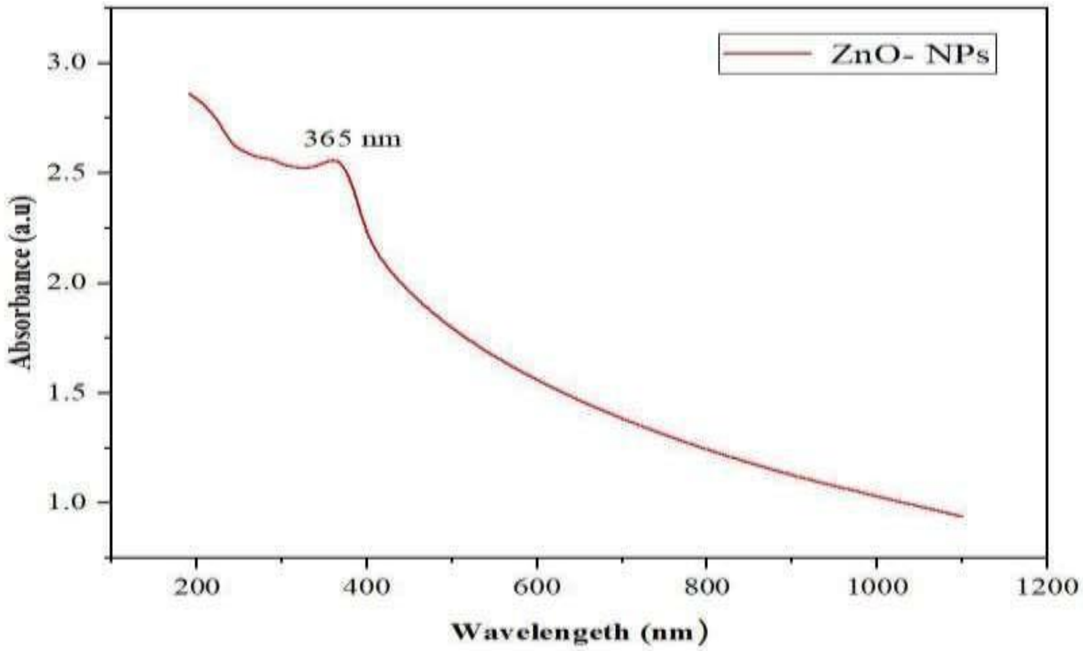

Figure27: UV-Visible Spectroscopy Analysis

This absorption band corresponds to the intrinsic electronic transition from the valence band to the conduction band of ZnO, and is considered a defining optical feature of semiconductor zinc oxide nanoparticles at the nanoscale. The sharp and well-defined absorption profile further suggests a relatively homogeneous particle size distribution and good optical purity of the synthesized material (Dulta et al., 2021; Singh et al., 2012).

The gradual decrease in absorbance toward the visible and near-infrared regions reflects the typical semiconducting behavior of ZnO and demonstrates its strong and selective interaction with ultraviolet radiation. Slight variations in absorption intensity or spectral profile compared to other studies may be attributed to differences in particle size distribution, degree of crystallinity, surface defects, oxygen vacancies, or the presence of residual phytochemical capping agents derived from *Daucus carota* seed extract. At the nanoscale, such factors can induce quantum confinement effects that modify the optical absorption behavior of the material (Singh et al., 2012).

The observed peak position is in close agreement with values reported by Dulta et al. (2021), who recorded a strong UV absorption band in the same spectral region for ZnO nanoparticles synthesized from *Carica* papaya leaf extract, and (with Singh et al. 2012), who identified a prominent absorption peak at 367 nm for ZnO nanoparticles. This consistency with the literature validates the nanoscale formation and optical stability of the prepared ZnO-NPs and confirms the effectiveness of the green synthesis approach adopted in the present study.

III.5. Anitbacterial Activity of *Daucus carota. L*

Antibacterial Activity of ZnO-NPs and Raw *Daucus carota* Seed Extract The antibacterial activity of both test samples was evaluated against 3 reference bacterial strains using the agar-well diffusion method. The diameters of inhibition zones (mm) were measured after 24 hours of incubation at 37°C. The negative control (5% DMSO) produced no inhibition zone in any experiment, confirming that the observed activity was solely attributable to the test samples. Results are summarized in Tables 4(1&2).

Table 1. *Inhibition zone diameters (mm) of green-synthesized ZnO-NPs (Sample R) against refere bacterial strains.*

Bacterial Strain	10 mg/mL	7.5 mg/mL	5 mg/mL	2.5 mg/mL	Neg. Cont
E. coli ATCC 25922	26	17	15	NI	NI
P. aeruginosa ATCC 27853	21	15	13	NI	NI
S. aureus ATCC 25932	29	24	19	14	NI

NI = No Inhibition

Table 2. *Inhibition zone diameters (mm) of raw Daucus carota seed extract (Sample R') against reference bacterial strains.*

Bacterial Strain	10 mg/mL	7.5 mg/mL	5 mg/mL	2.5 mg/mL	Neg. Cont
E. coli ATCC 25922	27	19	17	NI	NI
P. aeruginosa ATCC 27853	20	8	NI	NI	NI
S. aureus ATCC 25932	23	18	13	8	NI

The antibacterial evaluation of both test samples revealed a clear concentration-dependent inhibitory activity against all three reference strains. The green-synthesized ZnO nanoparticles (Sample R) demonstrated broad-spectrum antibacterial efficacy, with the largest inhibition zones recorded against *S. aureus* (29 mm at 10 mg mL-1), followed by *E. coli* (26 mm) and *P. aeruginosa* (21 mm) at the same concentration. Inhibitory activity was detectable down to 5 mg mL-1 for all strains, and persisted at 2.5 mg mL-1 exclusively against *S. aureus*, reflecting the dose-dependent nature of the antibacterial response (Abdelbaky et al., 2022).

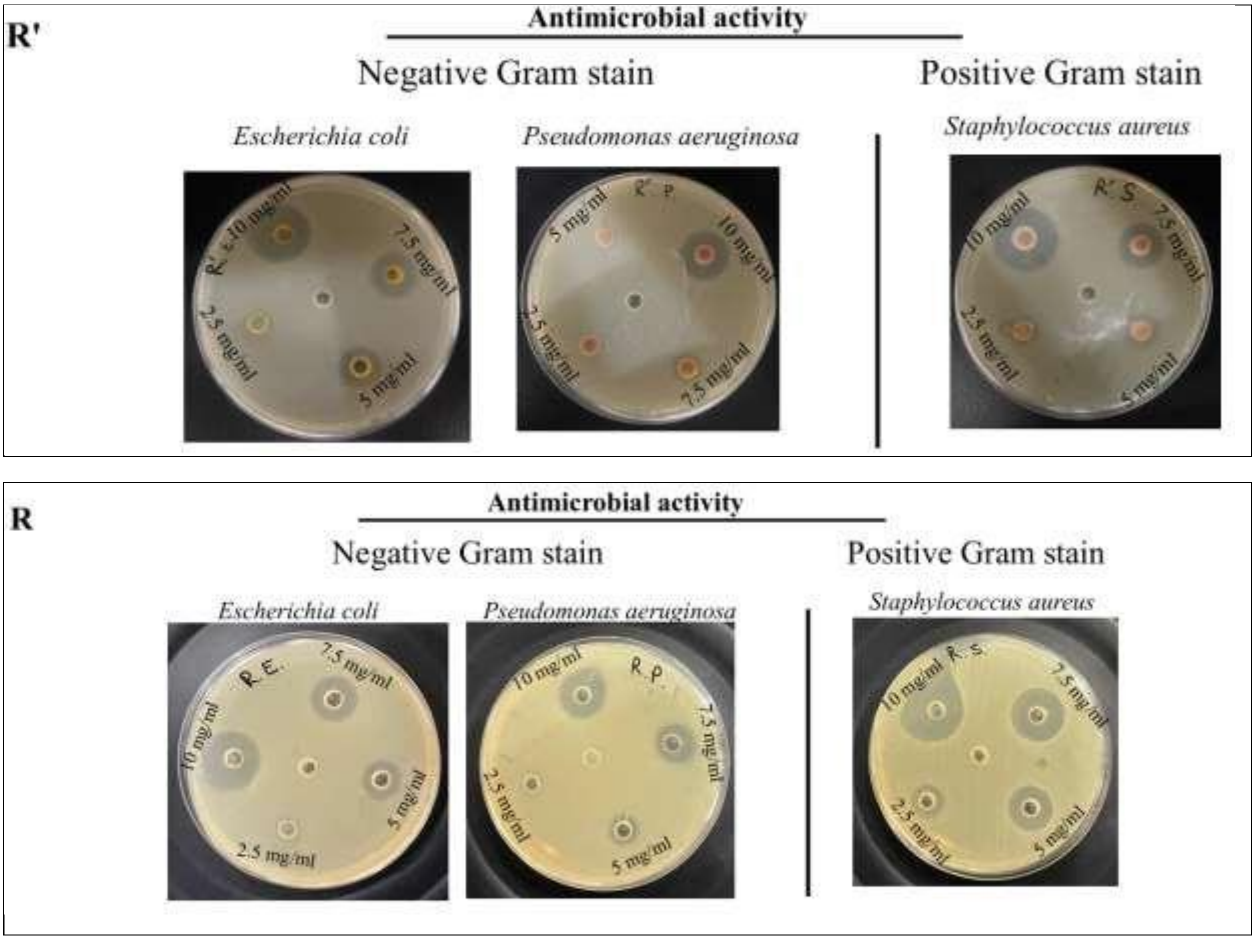

Figur28: Antibacterial Activity Assessment **(Original photo, 2026)**

The superior susceptibility of *S. aureus* compared to the two Gram-negative strains can be explained by fundamental structural differences in bacterial cell walls. Gram-negative bacteria possess an outer membrane composed of lipopolysaccharides that acts as an additional permeability barrier, limiting nanoparticle penetration and interaction with the inner membrane and cytoplasmic components. In contrast, the absence of this outer membrane in Gram-positive *S. aureus* renders it comparatively more accessible to nanoparticle-mediated disruption (Mulugeta & Wube, 2025). The particularly limited activity against *P. aeruginosa* below 7.5 mg mL-1 may further reflect the intrinsic resistance mechanisms of this species, including highly efficient efflux pump systems and biofilm-forming capacity (Selvaraj et al., 2024).

The raw methanolic extract of *Daucus carota L.* seeds (Sample R') also exhibited meaningful antibacterial activity, particularly at the highest concentration tested (10 mg mL-1), with inhibition zones of 27 mm against *E. coli* and 23 mm against *S. aureus*. However, activity against *P. aeruginosa* was restricted to concentrations above 7.5 mg mL-1 and was absent at lower concentrations, highlighting the limited potency of the raw extract against this resistant species. These results are consistent with the known antimicrobial properties of *Daucus carota* seed phytochemicals, including flavonoids, phenolic acids, and isothiocyanates (Nicolle et al., 2017).

A direct comparison between Samples R and R' reveals that the ZnO-NPs displayed broader and more consistent antibacterial activity across all tested concentrations and strains. In particular, Sample R maintained measurable inhibition against *P. aeruginosa* at 5 mg mL-1 (13 mm), whereas Sample R' showed no detectable activity at and below this concentration for the same strain. This enhancement may be attributed to a synergistic interaction between the ZnO nanoparticle core and the phytochemical capping agents derived from the seed extract, which not only stabilize the nanoparticles but likely facilitate their adhesion to and penetration of bacterial membranes, thereby amplifying the overall antibacterial efficacy beyond what either component achieves independently (Pasieczna-Patkowska et al., 2025; Shaheen et al., 2024).

III.6. The Sun Protection Factor (SPF) Results:

Using Mansur formulation our experimental results gave an SPF value of:

Sample R (ZnO-NPs): SPF = 10 × 1.74753 ≈ 17.48

Sample R' (Carrot extract): SPF = 10 × 1.90593 ≈ 19.06

Table 5. Correlation between erythemogenic effect (EE × I) and absorbance values at each wavelength for Sample R and Sample R'

λ (nm)	EE (λ) × I (λ)	A (λ) — Sample R	A (λ) Sample R'	EE×I×A Sample R	EE×I×A Sample R'
290	0.0150	1.165	1.408	0.01748	0.02112
295	0.0817	1.474	1.715	0.12043	0.14012
300	0.2874	1.759	1.897	0.50554	0.54520
305	0.3278	1.786	1.950	0.58545	0.63921
310	0.1864	1.795	1.925	0.33459	0.35882

λ (nm)	EE (λ) × I (λ)	A (λ) — Sample R	A (λ) Sample R'	EE×I×A Sample R	EE×I×A Sample R'
315	0.0839	1.820	1.996	0.15270	0.16746
320	0.0180	1.742	1.889	0.03136	0.03400
∑				**1.74753**	**1.90593**

The SPF values obtained for ZnO nanoparticles (17.469) and carrot seed extract (19.047) indicate that both materials possess significant photoprotective activity. Although ZnO nanoparticles exhibited a slightly higher SPF value, the difference between the two samples was relatively small. These findings suggest that carrot seed extract can contribute effectively to UV protection, probably due to its content of antioxidant compounds such as phenolics and flavonoids. The results also confirm the well-established UV-screening properties of ZnO nanoparticles. Therefore, the combination of carrot seed extract and ZnO nanoparticles may represent a promising strategy for developing sunscreen formulations with enhanced photoprotective efficacy.

Discussion

The extraction yield of 9.99% obtained from the mthanolic extraction of *Daucus carota L.* seeds confirmed the richness of this plant matrix in soluble bioactive compounds. The subsequent phytochemical characterization revealed that phenolic compounds constituted the dominant class, followed by tannins and flavonoids in progressively lower quantities.

This distribution is fully consistent with the phytochemical profile previously reported for *Daucus carota* seeds by Ismail et al. (2024), who identified phenolic acids and polyphenols as the principal secondary metabolites of this species, and is further supported by the findings of Akhtar et al. (2023), who demonstrated comparable phytochemical hierarchies in carrot seed extracts prepared under similar extraction conditions. The predominance of phenolic compounds is of direct relevance to the green synthesis process, as these molecules are well recognized for their dual capacity to reduce zinc ions and simultaneously stabilize the forming nanoparticles through surface capping, thereby guiding particle growth and preventing excessive aggregation (Miu & Dinischiotu, 2022; Ansari et al., 2024).

The extraction process yielded a 9.99% recovery rate (0.1997 g of crude extract from 2g of dry plant matter), establishing a solid quantitative foundation for subsequent biochemical analysis. Quantitative phytochemical characterization revealed a distinct hierarchy among the secondary metabolites, where Total Phenolic Content (TPC) emerged as the dominant component at approximately 1.5 mg/g of dry matter (via gallic acid curve, Total Flavonoid Content (TFC) was detected in moderate amounts at 0.4

mg/g (via quercetin curve, while Total Tannin Content (TTC) represented the smallest fraction at 0.1 mg/g (via tannic acid curve. This distribution strongly suggests that the extract's matrix is structurally dominated by low-molecular-weight phenolic acids. These specific chemical groups possess highly accessible hydroxyl groups, which serve as the primary drivers for electron-transfer and free radical stabilization.

The antioxidant capacity of the samples was evaluated using the DPPH assay, and all tested groups demonstrated a clear, dose-dependent radical scavenging response. The antioxidant potency was quantified using CI50 values, where a lower concentration reflects superior scavenging efficiency. As an optimized pure compound, the Ascorbic Acid reference standard exhibited the highest potency with an CI50 of 5.30 µg/ml. The crude plant extract displayed a steady, linear escalation in radical scavenging activity climbing from 5% inhibition at 3.35 µg/ml up to 58% at 80 µg/ml resulting in an calculated CI of 70.67 µg/ml. Crucially, the synthesized zinc oxide nanoparticles (ZnO-NPs) demonstrated an intermediate, highly substantial antioxidant capacity with an CI value of 22.16 µg/ml, verifying their potential efficacy for targeted biomedical and pharmaceutical applications.

A comparative analysis of these functional kinetics reveals that the ZnO-NPs are approximately 3.2 times more potent than the crude plant extract alone, illustrating a highly successful green nanotechnology synthesis. During the formation of the nanomaterial, the abundant phenolics and flavonoids present in the plant matrix act as natural reducing and capping agents. By binding directly to the developing zinc cores, these active phytoconstituents become densely concentrated onto a crystalline lattice with an exceptionally high surface-area-to-volume ratio.

This localized alignment triggers a mechanistic synergy, combining the rapid electron-transfer kinetics of the metallic oxide surface with the concentrated hydrogen-donating capacity of the plant's surface-bound polyphenols. Consequently, the nano-formulation effectively bridges the performance gap between raw botanical fractions and pure ascorbic acid, validating this green synthesis method as an efficient strategy for producing biocompatible materials with enhanced antioxidant properties.

The structural and optical characterization of the synthesized nanoparticles provided convergent and unambiguous confirmation of successful ZnO formation. The XRD analysis established a phase-pure hexagonal wurtzite crystalline structure, with all diffraction peaks perfectly matching the standard ZnO reference pattern and no secondary phase reflections detected. The high crystallinity of the product, evidenced by the sharpness of the peaks and the dominance of the (101) reflection, is largely attributable to the calcination step at 600°C, which eliminated residual organic matter and promoted the ordering of the crystalline lattice (Naqvi et al., 2011; Zidi et al., 2020).

The FTIR analysis provided additional and complementary confirmation of the structural findings obtained from XRD and UV–Visible spectroscopy. The intense absorption band detected below 600 cm^{-1}, particularly within the 400–500 cm^{-1} region, was assigned to the characteristic Zn–O stretching vibration, consistent with values reported in comparable green synthesis studies employing plant extracts as bioreducing agents (Vinotha et al., 2019; Yadav et al., 2022). The presence of this fingerprint band corroborates the phase-pure hexagonal wurtzite structure established by XRD and confirms that the calcination step successfully converted the zinc precursor into crystalline ZnO.

In parallel, the moderate absorption band observed around 1000–1100 cm^{-1}, attributed to C–O stretching vibrations of phenolic and carbohydrate-related functional groups, together with the comparatively weak residual organic signals in the higher wavenumber region, indicates that the phytochemicals of the carrot seed extract were largely consumed during the bioreduction and capping process while leaving only limited organic residues following thermal treatment.

These findings reinforce the conclusions drawn from the UV–Visible absorption peak at 365 nm, as the limited surface organic content is consistent with the relatively narrow and well-defined optical absorption profile observed, reflecting a homogeneous and low-defect nanoparticle population. Taken together, the convergent evidence from XRD, UV–Visible spectroscopy, and FTIR analysis confirms that the phytochemical-mediated green synthesis protocol successfully produced crystalline, phase-pure, and surface-functionalized ZnO nanoparticles.

These structural findings were fully corroborated by the UV–Visible spectroscopic data, which showed a characteristic absorption peak at 365 nm, a value in close agreement with those reported by Dulta et al. (2021) and Singh et al. (2012) for ZnO-NPs produced through comparable green synthesis routes, confirming that the phytochemical-mediated approach successfully directed the formation of optically active and crystalline nanostructures.

The biological evaluations demonstrated a consistent and meaningful functional advantage of the biosynthesized ZnO-NPs over the raw seed extract. In the antibacterial assessment, Sample R produced broader and more potent inhibition across all tested strains and concentrations, with *S. aureus* exhibiting the highest susceptibility among the three organisms tested. This pattern is explained by the structural vulnerability of Gram-positive bacteria, which lack the outer lipopolysaccharide membrane that in *E. coli* and particularly *P. aeruginosa* acts as an additional permeability barrier limiting nanoparticle penetration (Mulugeta & Wube, 2025; Selvaraj et al., 2024).

The superior performance of Sample R relative to Sample R' reflects a synergistic interaction between the ZnO core which generates reactive oxygen species and disrupts membrane integrity and the phytochemical capping layer, which facilitates nanoparticle adhesion to bacterial surfaces and independently contributes antimicrobial activity (Shaheen et al., 2024; Abdelbaky et al., 2022). A comparable advantage was observed in the antioxidant assessment, where the ZnO-NPs demonstrated stronger DPPH radical scavenging activity than the extract alone, attributable to the combined electron-transfer capacity of surface oxygen vacancies in the ZnO core and the retained phenolic capping agents (Abdelbaky et al., 2022; Dziri et al., 2012).

The photoprotective evaluation confirmed that the incorporation of biosynthesized ZnO-NPs into the sunscreen formulation yielded a meaningful SPF value of 19.047, slightly exceeding that of the extract alone (17.469), in line with the broad-spectrum UV-filtering properties of ZnO arising from its wide band gap and high refractive index (Nikam et al., 2023).

The skin-compatible pH of the final cream formulation further supports the practical suitability of this preparation for topical cosmetic application, and collectively the results of this study confirm that *Daucus carota L.* seeds represent a promising and sustainable bioresource for the green synthesis of multifunctional ZnO nanoparticles with genuine potential in cosmetic and pharmaceutical formulations (Miloudi et al., 2025; Haiouani et al., 2024).

Conclusion

Conclusion

This study demonstrates that the plant extract is an effective bio-reducer rich in phenolic compounds. Converting this raw botanical extract into a nano-formulation (ZnO-NPs) substantially optimizes its radical-scavenging performance. These findings confirm the value of the extract as a starting material for green nanotechnology, yielding functional nanoparticles with promising application potential in antioxidant therapies and biomedical engineering.

The results obtained throughout this study confirm that the green synthesis protocol adopted was effective in producing crystalline, pure, and optically active ZnO-NPs, as demonstrated by the convergent findings of UV-Visible spectroscopy, XRD, and FTIR characterization. The phytochemical richness of the seed extract, particularly in phenolic compounds, not only facilitated the bioreduction and stabilization of the nanoparticles but also contributed to their biological activity.

The biological assessments conducted in this study, encompassing antibacterial and antioxidant evaluations, demonstrated that the biosynthesized ZnO-NPs possessed superior and broader biological activity compared to the raw seed extract, suggesting a meaningful synergistic contribution of the nanoparticle structure and the phytochemical surface agents. Furthermore, the incorporation of ZnO-NPs into a cream formulation yielded a stable sunscreen product with satisfactory photoprotective properties and skin-compatible pH values.

Evaluation of its photoprotective activity revealed that the *Daucus carota L.* seed extract provides high sun protection against UVB ray (SPF +20). This research led to the development of a sunscreen made with mostly natural ingredients, showing promising potential in the parapharmaceutical field. Indeed, this cream offers high antioxidant, photoprotective, and antibacterial protection.

Collectively, the present findings confirm that *Daucus carota L.* seeds represent a promising and renewable biological resource for the green synthesis of multifunctional ZnO nanoparticles, and that the resulting nanomaterial holds real potential for integration into future cosmetic and pharmaceutical formulations. These results open perspectives for further investigations aimed at optimizing synthesis conditions, deepening structural characterization, and conducting in vivo safety and efficacy assessments.

References

References

1. Abdelbaky, A. S., Abd El-Mageed, T. A., Babalghith, A. O., Selim, S., & Mohamed, A. M. H. A. (2022). Green synthesis and characterization of ZnO nanoparticles using Pelargonium odoratissimum (L.) aqueous leaf extract and their antioxidant, antibacterial and anti-inflammatory activities. Antioxidants, 11(8), 1444. https://doi.org/10.3390/antiox11081444
2. Abdelhakim, H. K., El-Sayed, E. R., & Rashidi, F. B. (2020). Biosynthesis of zinc oxide nanoparticles with antimicrobial, anticancer, antioxidant and photocatalytic activities by the endophytic Alternaria tenuissima. Journal of Applied Microbiology, 128(6), 1634–1646. Portico.https://doi.org/10.1111/jam.14581
3. Abegunde, S. M., et al. (2025). Eco-friendly nanoparticle phytosynthesis via plant extracts: Mechanistic insights, recent advances, and multifaceted uses. Green Analytical Chemistry.https://doi.org/10.1016/j.greeac.2025.100
4. ،Ahmad, T., Cawood, M., Iqbal, Q., Ariño, A., Batool, A., Tariq, R. M. S., Azam, MAkhta,S. Review article. Foods —Phytochemicals in Daucus carota and their health benefits .(2019)
5. Akhtar, I., Javad, S., Jabeen, K., Saddiqe, Z., Shah, A., & Aslam, F. (2023). A rapid recovery of phytochemicals from carrot seeds: an analytical approach. Journal of Taibah University for Science, 17. https://doi.org/10.1080/16583655.2023.2221051.
6. Ali, S. A., Khan, W., Chaman, M., & Naqvi, A. H. (2011). Synthesis, structural and optical properties of Cr doped ZnO nanoparticles. Asian Journal of Chemistry, 23(12), 5622–5624.
7. Ansari, M. A., et al. (2024). A review on plant extract mediated green synthesis of zinc oxide nanoparticles and their biomedical applications. Biomedicine & Pharmacotherapy, 172, 116204. https://doi.org/10.1016/j.biopha.2024.116204
8. Arias, L. S., Pessan, J. P., Vieira, A. P. M., Lima, T. M. T., Delbem, A. C. B., & Monteiro, D. R. (2022). Iron oxide nanoparticles for biomedical applications: A perspective on synthesis, drugs, antimicrobial activity, and toxicity. Antibiotics, 11(3), 368. https://doi.org/10.3390/antibiotics11030368
9. Ayoub, I., Kumar, V., Abolhassani, R., Sehgal, R., Sharma, V. S., Sehgal, R., Swart, H., & Mishra, Y. (2022). Advances in ZnO: Manipulation of defects for enhancing their technological potentials. Nanotechnology Reviews, 11, 575 - 619. https://doi.org/10.1515/ntrev-2022-0035
10. Ayub, A., Wani, A., Malik, S., Ayub, M., Singh, R., Chopra, C., & Malik, T. (2025). Green nanoscience for healthcare: Advancing biomedical innovation through eco-synthesized nanoparticle. Biotechnology Reports, 47. https://doi.org/10.1016/j.btre.2025.e00913.

11. Baig, N., Kammakakam, I., & Falath, W. (2025). Nanomaterials: A review of synthesis methods, properties, recent progress, and challenges. Materials Advances, 6(1), 1–25. https://doi.org/10.1039/D0MA00807A
12. Baumberg, J., & Baumberg, C. (2024). The emergence of nanoscience. Journal of Physics: Conference Series, 2877. https://doi.org/10.1088/1742-6596/2877/1/012094.
13. Benhammou, N., Bekkara, F. A., & Panovska, T. K. (2009). Antioxidant and antimicrobial activities of the Pistacia lentiscus and Pistacia atlantica extracts. African Journal of Pharmacy and Pharmacology, 3(5), 501–509.
14. Bhattacharya, S., & Sherje, A. P. (2020). Development of resveratrol and green tea sunscreen formulation for combined photoprotective and antioxidant properties. Journal of Drug Delivery Science and Technology, 60, 102000. https://doi.org/10.1016/j.jddst.2020.102000
15. Biomedical applications. Nanomaterials, 12(17), 3066. https://doi.org/10.3390/nano12173066
16. Bipinchandra, P., Hiteshbhai, P., & Shrivastava, V. (2025). A review on formulation and evaluation of sunscreen. International Journal for Multidisciplinary Research.https://doi.org/10.36948/ijfmr.2025.v07i02.40450
17. Bonev, B., Hooper, J., & Parisot, J. (2008). Principles of assessing bacterial susceptibility to antibiotics using the agar diffusion method. *Journal of antimicrobial chemotherapy*, *61*(6), 1295-1301.
18. Borysiewicz, M. (2019). ZnO as a Functional Material, a Review. Crystals. https://doi.org/10.3390/cryst9100505
19. CABI. (2022). Daucus carota (carrot). CABI Compendium. https://www.cabidigitallibrary.org/doi/abs/10.1079/cabicompendium.18018
20. Carniel, L., Gomes, M., Bazzo, G. C., Ribeiro, H., Marto, J., & Pezzini, B. R. (2025). Rational QbD-based assessment of formulation ingredients' impact on sustainable sunscreen physical stability. AAPS PharmSciTech, 26. https://doi.org/10.1208/s12249-025-03192-7
21. Cervantes-a synthesis of ZnO nanoparticles using Sorghum bicolor seed extract and their application in photocatalytic dye degradation. Chemengineering, 8(1), 15. https://doi.org/10.3390/chemengineering10010015
22. Cvetković, D., Stanojević, L., Ilić, Z. S., Tmušić, N., Stanković, J., & Šunić, L. (2023). Essential oil yield, composition, and antioxidant activity in two umbel maturity stages of wild carrot (Daucus carota L. ssp. carota) from Montenegro. Horticulturae, 9(3), 328.https://doi.org/10.3390/horticulturae9030328

23. Deshmukh, S. P., Shrivastava, J. A., & Bhajipale, N. S. (2021). A review: Pharmacological actions of Daucus carota. International Journal of Pharmacy and Pharmaceutical Research, 21(2), 302–314. https://ijppr.humanjournals.com
24. Dziri, S., Hassen, I., Fatnassi, S., Mrabet, Y., Casabianca, H., Hanchi, B., & Hosni, K. (2012). Phenolic constituents, antioxidant and antimicrobial activities of rosy garlic (Allium roseum var. odoratissimum). Journal of Functional Foods, 4(2), 423–432. https://doi.org/10.1016/j.jff.2012.02.003
25. Eid, M. M. (2022). Characterization of nanoparticles by FTIR and FTIR-microscopy. In Handbook of Consumer Nanoproducts. Springer. https://doi.org/10.1007/978-981-16-8698-6_89
26. El-Seedi, H., El-Shabasy, R. M., Khalifa, S., Saeed, A., Shah, A., Shah, R., Iftikhar, F. J., Abdel-Daim, M. M., Omri, A., Hajrahand, N. H., Sabir, J., Zou, X., Halabi, M. F., Sarhan, W., & Guo, W. (2019). Metal nanoparticles fabricated by green chemistry using natural extracts: biosynthesis, mechanisms, and applications. RSC Advances, 9, 24539 - 24559.https://doi.org/10.1039/c9ra02225b
27. Ersoy, E., Batal Yıldızhan, R., Yılmaz, M. A., Yeşil, Y., Şahin, H., Eroğlu Özkan, E., & Boğa, M. (2024). Investigating the pharmacological potential of Micromeria myrtifolia Boiss. & Hohen.: Phenolic profiling and biological activity assessments. Commagene Journal of Biology, 8(2), 103–114. https://doi.org/10.31594/commagene.1576852
28. Ghellab, A.H., et al., Optimization of operating conditions for the green synthesis of ZnO, CuO, and ZnO-CuO nanoparticles and nanocomposites. 2023
29. Green renewable resources and energy-efficient synthetic routes. Nanotechnology Reviews, 11, 731 - 759. https://doi.org/10.1515/ntrev-2022-0034
30. Haiouani, K., Hegazy, S., Alsaeedi, H., Bechelany, M., & Barhoum, A. (2024). Green synthesis of hexagonal-like ZnO nanoparticles modified with phytochemicals of clove and Thymus capitatus extracts: Enhanced antibacterial, antifungal, and antioxidant activities. Materials, 17(17), 4340. https://doi.org/10.3390/ma17174340
31. Hameed, A., Akram, N., Saleem, M., Ashraf, M., Ahmed, S., Ali, S., Alsahli, A., & Alyemeni, M. (2021). Seed Treatment with α-Tocopherol Regulates Growth and Key Physio-Biochemical Attributes in Carrot (Daucus carota L.) Plants under Water Limited Regimes. Agronomy.https://doi.org/10.3390/agronomy11030469.
32. Hammad, E. N., Mahmoud, A. K., & Abdelaziz, A. M. (2022). Green synthesis and characterization of zinc oxide nanoparticles: A comprehensive review of their biological applications. Journal of Inorganic and Organometallic Polymers and Materials.

33. Hughes, K. J., Ganesan, M., Tenchov, R., Iyer, K. A., Ralhan, K., Diaz, L. L., Bird, R. E., Ivanov, J., & Zhou, Q. A. (2025). Nanoscience in action: Unveiling emerging trends in materials and applications. ACS Omega, 10(8), 7530–754
34. International Journal of Scientific Research and Reviews, 8(2), 2700–2715.
35. Ismail, J., Shebaby, W. N., Daher, J., Boulos, J. C., Taleb, R., Daher, C. F., & Mroueh, M. (2024). The wild carrot (Daucus carota): A phytochemical and pharmacological review. Plants, 13(1), 93.https://doi.org/10.3390/plants13010093
36. Joudeh, N., & Linke, D. (2022). Nanoparticle classification, physicochemical properties, characterization, and applications: a comprehensive review for biologists. Journal of Nanobiotechnology, 20. https://doi.org/10.1186/s12951-022-01477-8
37. Khan, Y., Sadia, H., Shah, S., Khan, M., Shah, A., Ullah, N., Ullah, M., Bibi, H., Bafakeeh, O., Khedher, N., Eldin, S., Fadhl, B., & Khan, M. (2022). Classification, Synthetic, and Characterization Approaches to Nanoparticles, and Their Applications in Various Fields of Nanotechnology: A Review. Catalysts. https://doi.org/10.3390/catal12111386.
38. Kiehlbauch, J. A., Hannett, G. E., Salfinger, M., Archinal, W., Monserrat, C., & Carlyn, C. (2000). Use of the National Committee for Clinical Laboratory Standards guidelines for disk diffusion susceptibility testing in New York state laboratories. *Journal of clinical microbiology*, *38*(9), 3341-3348.
39. Kiriiri, G. K., Njogu, P. M., & Mwangi, A. N. (2019). Exploring different approaches to improve the success of drug discovery and development projects: A review. Future Journal of Pharmaceutical Sciences, 5(1), 20. https://doi.org/10.1186/s43094-019-0020-2
40. Koley, T. K., Khan, Z., Oulkar, D., Bhatt, R., & Bhattacharya, S. (2022). Carrot (Daucus carota L.): nutritional composition and nutritional interventions. Frontiers in Nutrition, 9, 900282. Koley, T. K., Khan, Z., Oulkar, D., Bhatt, R., & Bhattacharya, S. (2022). Carrot (Daucus carota L.): nutritional composition and nutritional interventions. Frontiers in Nutrition, 9, 900282. https://doi.org/10.3389/fnut.2022.900282
41. Kulawik-Pióro, A. (2022). Carrot (Daucus carota L.) as a source of active substances and its pharmacological and cosmetology potential. Farmacja Polska, 78(9), 536–548.https://doi.org/10.32383/farmpol/156891
42. Luque, P. A., Nava, O., Soto-Robles, C. A., et al. (2018). Effects of Daucus carota extract used in green synthesis of zinc oxide nanoparticles. Journal of Materials Science: Materials in Electronics, 29, 17638–17643. https://doi.org/10.1007/s10854-018-9867-5
43. Madani, M., Hosny, S., Alshangiti, D., Nady, N., Alkhursani, S., Alkhaldi, H., Al-Gahtany, S., Ghobashy, M., & Gaber, G. (2022). Green synthesis of nanoparticles for varied applications:

44. Malaiappan, S., Murugesan, S., Krishnamurthy, S., & Arumugam, P. (2024). Green synthesis and characterization of zinc oxide nanoparticles using Catharanthus roseus extract: A novel approach. Cureus, 16(5), e61234. https://doi.org/10.7759/cureus.61234
45. Mandal, A. K., Katuwal, S., Tettey, F., Gupta, A., Bhatt, S., Bhatt, N., Adhikari, S., & Bhatt, M. D. (2022). Current research on zinc oxide nanoparticles: Synthesis, characterization, and biomedical applications. Nanomaterials, 12(17), 3066. https://doi.org/10.3390/nano12173066
46. Mansur, J. S., Breder, M. N. R., Mansur, M. C. A., & Azulay, R. D. (1986). Determinação do fator de proteção solar por espectrofotometria. Anais Brasileiros de Dermatologia, 61(3), 121–124.
47. Mekuye, B., & Abera, B. (2023). Nanomaterials: An overview of synthesis, classification, characterization, and applications. *Nano Select*, *4*(8), 486 501 . https://doi.org/10.1002/nano.202300038
48. Miloudi, H., Zaoui, A., & Zedik, Y. (2025). In vitro study on the biological activities of Ammodaucus leucotrichus Zn-O nanoparticles, essential oil and hydroethanolic extract [Master's thesis, Echahid Hamma Lakhdar University of El-Oued].
49. MIu, B., & Dinischiotu, A. (2022). New Green Approaches in Nanoparticles Synthesis: An Overview. Molecules, 27. https://doi.org/10.3390/molecules27196472
50. Mohamad Sukri, S. N. A., Shameli, K., Teow, S. Y., Chew, J., Ooi, L. T., Soon, M. L. K., Ismail, N. A., & Moeini, H. (2023). Enhanced antibacterial and anticancer activities of plant extract mediated green synthesized zinc oxide-silver nanoparticles. Frontiers in Microbiology, 14, 1194292. https://doi.org/10.3389/fmicb.2023.1194292
51. Mughal, T. A., Abid, U., Saddiq, Z., Naseeb, S., & Pervaiz, S. (2018). Qualitative and quantitative evaluation of tannins in bark extracts of some indigenous plants of Pakistan. International Chutulo, E. C., Chalannavar, R. K., & Kumar, P. P. (2020). Chemical compositions, cytotoxicity and antioxidant activity of the endophytic fungus Fusarium napiforme isolated from Psidium guajava. Studies in Fungi, 5(1), 332–352. https://doi.org/10.5943/sif/5/1/15 Journal of Biosciences, 12(6), 78–84. https://doi.org/10.12692/ijb/12.6.78-84
52. Mulugeta, M., & Wube, T. (2025). Synthesis of zinc oxide nanoparticles using the leaves extract of Rhamnus prinoides and its antibacterial activities. Discover Applied Sciences. https://doi.org/10.1007/s42452-025-07669-9
53. Nasiruddin, M., & Sinha, S. N. (2020). Phytochemical screening and antioxidant, antibacterial efficacy of Gynura procumbens (Lour.) Merr. Asian Journal of Medical and Biological Research, 6(2), 187–195. https://doi.org/10.3329/ajmbr.v6i2.48049
54. Nikam, B., Deokar, N. P., Varsha, J., & Arora, M. (2023). Efficacy of topical nanoparticle-based sunscreens in UV protection. Journal of Chemical Health Risks, 13(2s).

55. Osterwalder, U., & Herzog, B. (2009). Sun protection factors: world wide confusion. British Journal of Dermatology, 161(s3), 13–24. https://doi.org/10.1111/j.1365-2133.2009.09506.x
56. Pasieczna-Patkowska, S., Cichy, M., & Flieger, J. (2025). Application of Fourier Transform Infrared (FTIR) spectroscopy in characterization of green synthesized nanoparticles. Molecules, 30(3), 684. https://doi.org/10.3390/molecules30030684
57. Rajput, J., & KashishSaroj,. (2025). Nanotechnology in Modern Physics: Materials, Devices, and Applications. International Journal of Advanced Research and Interdisciplinary Scientific Riaz, N., Yousaf, Z., Yasmin, Z., Munawar, M., Younas, A., & Rashid, M. (2023). A rapid recovery of phytochemicals from carrot seeds: an analytical approach. Journal of King Saud University – Science, 35(6). https://doi.org/10.1080/16583655.2023.2221051
58. Results & Discussion — Antibacterial Activity Page 2 Nicolle, C., Simon, G., Rock, E., Amouroux, P., & Rémésy, C. (2017). Nutritional and therapeutic importance of Daucus carota — A review. African Journal of Biomedical Research, 20, 1–10. Pasieczna-Patkowska, S., Cichy, M., & Flieger, J. (2025). Application of Fourier Transform Infrared (FTIR) spectroscopy in characterization of green synthesized nanoparticles. Molecules, 30(3), 684. https://doi.org/10.3390/molecules30030684
59. Sahib, H. B., Jawad, A. H., & Kadhim, M. J. (2022). Medicinal properties of Daucus carota in traditional Persian medicine and modern phytotherapy. Journal of Biochemical Technology, 13(2), 1–9.
60. Santos, Y. R., Andréo-Filho, N., Lopes, P. S., Araujo, D., Sepulveda, A. F., Sales, C., Baby, A., Duque, M. D., & Leite-Silva, V. R. (2025). The influence of complementary processing methods to emulsification on the sunscreen emulsion properties. Processes, 13(2), 520.https://doi.org/10.3390/pr13020520
61. Saxena, R., Kotnala, S., Bhatt, S., Uniyal, M., Rawat, B., Negi, P., & Riyal, M. (2025). A REVIEW ON GREEN SYNTHESIS OF NANOPARTICLES TOWARD SUSTAINABLE ENVIRONMENT. Sustainable Chemistry for Climate Action.https://doi.org/10.1016/j.scca.2025.100071.
62. Sayeem, A., Rahman, M. M., Islam, M. S., Hossain, M. A., & Alam, M. K. (2026). Multifunctional applications of zinc oxide nanoparticles in agriculture, environment, and biomedicine: A comprehensive review. Journal of Nanobiotechnology, 24(1), 1–32. https://doi.org/10.1186/s12951-026-00001-0
63. Selvaraj, R., Krishnaswamy, S., & Vasantha, V. S. (2024). Harnessing biological synthesis: Zin oxide nanoparticles for plant biotic stress management. Frontiers in Chemistry, 12, 1432469. https://doi.org/10.3389/fchem.2024.1432469

64. Shaheen, T. I., et al. (2024). Phytogenic-mediated zinc oxide nanoparticles using the seed extract of Citrullus lanatus and its integrated potency against multidrug resistant bacteria. ACS Omega. https://doi.org/10.1021/acsomega.4c01554

65. Sim, S., & Wong, N. (2021). Nanotechnology and its use in imaging and drug delivery (Review).. Biomedical reports, 14 5, 42 . https://doi.org/10.3892/br.2021.1418.

66. Simon, P. W., Freeman, R. E., Vieira, J. V., Boiteux, L. S., Briard, M., Nothnagel, T., & Grzebelus, D. (2023). Carrot. In Vegetables I (pp. 327–357).

67. Sing, K., Dhongade, H., Sing, N. and Kashyap, P. (2010) Hypolipidemic Activity of Ethanolic Extract of Daucus carota Seeds in Normal Rats. International Journal of Biomedical and Advance Research, 1, 73-80

68. Soare, L. C., Ferdes, M., Stefanova, R., Stefanov, S., Neagu, G., & Avramescu, S. M. (1997). Antioxidant activity of some plant extracts. Journal of Agroalimentary Processes and Technologies, 13(2), 511–516.

69. Špaglová, M., Čermáková, P., Jackuliaková, P., & Piešťanský, J. (2025). Role of emulsifiers and SPF booster in sunscreen performance: Assessing SPF, rheological behavior, texture, and stability. Cosmetics, 12(3), 118. https://doi.org/10.3390/cosmetics12030118

70. Sportelli, M. C., Ancona, A., Trapani, A., Picca, R. A., Bonerba, E., Lippolis, V., Cioffi, N., & Conte, A. (2022). Zinc oxide nanoparticles for the prevention of COVID-19 and other viral respiratory diseases: A review. Frontiers in Bioengineering and Biotechnology, 10, 945048. https://doi.org/10.3389/fbioe.2022.945048

71. Sreelatha, S., & Inbavalli, R. (2012). Antioxidant, antihyperglycemic, and antihyperlipidemic effects of Coriandrum sativum leaf and stem in alloxan-induced diabetic rats. Journal of Food Science, 77(7), T119–T123. https://doi.org/10.1111/j.1750-3841.2012.02755.

72. Stanojević, J., Ilić, Z. S., Stanojević, L., Milenković, L., Kovač, R., Lalević, D., Šunić, L., Milenković, A., & Cvetković, D. (2023). Essential oil yield, composition, and antioxidant activity in two umbel maturity stages of wild carrot (Daucus carota L. ssp. carota) from Montenegro. Horticulturae, 9(3), 328. https://doi.org/10.3390/horticulturae9030328

73. Touahriya, S. A., & Said, H. (2021). Contribution to the morphophysiological and phytochemical study of leaves of olive (Olea europaea L.) cultivars grown in different geographical regions (Master's thesis, University of El Oued, Algeria).

74. Tran, H. V., et al. (2025). Green synthesis of iron oxide nanoparticles from extracts of Daucus carota subsp. sativus whole vegetable, peel, pomace, and juice and their application as antibacterial agents and Fenton-like catalysts. International Journal of Food Science and Technology, 60(1).https://doi.org/10.1093/ijfst/vvae035

75. Valtsifer, V., Sivtseva, A. V., Kondrashova, N., Shamsutdinov, A., Averkina, A. S., Valtsifer, I., Feklistova, I. N., & Strelnikov, V. N. (2023). Influence of Synthesis Conditions on the Properties of Zinc Oxide Obtained in the Presence of Nonionic Structure-Forming Compounds. Nanomaterials, 13. https://doi.org/10.3390/nano13182537
76. Vinotha, V., Anbu Selvam, A., Tamilarasan, K., & Babu, J. (2019). Green synthesis and characterization of zinc oxide nanoparticles using Cayratia pedata leaf extract. Biocatalysis and Agricultural Biotechnology, 24, 101541. https://doi.org/10.1016/j.bcab.2019.101541
77. Vyas, J. (2020). A review on zinc oxide nanoparticles: Synthesis, properties, and applications. International Journal of Scientific Research and Reviews, 8(2), 2700–2715.
78. Wang, Q., Zhang, H., Han, Y., Cui, Y., & Han, X. (2023). Study on the relationships between the oil HLB value and emulsion stabilization. RSC Advances, 13, 24692–24698.https://doi.org/10.1039/d3ra04592g
79. Y. (2022). Advances in ZnO: Manipulation of defects for enhancing their technological 0035-2022-https://doi.org/10.1515/ntrev .619 - 575 ‹1Nanotechnology Reviews, 1 potentials.
80. Yadav, S., Jain, R., Singh, S. P., & Sharma, S. (2022). Green synthesis of zinc oxide (ZnO) nanoparticles using aqueous fruit extracts of Myristica fragrans: Their characterizations and biological and environmental applications. ACS Omega, 7(13), 11500–11512. https://doi.org/10.1021/acsomega.1c00310
81. Yang, S., Liu, C., Kang, S., Brewer, A., Girolami, G., Chan, M., Klie, R., Chen, Q., Park, J., & Alivisatos, A. (2025). Precision nanoscience aided by multimodal observations. MRS Bulletin, 50, 1325 - 1340. https://doi.org/10.1557/s43577-025-00958-z.
82. Zidi, Z., Ltifi, M., Ben Ayadi, Z., El Mir, L., & Nóvoa, X. R. (2020). Effect of nano-ZnO on mechanical and thermal properties of geopolymer. Journal of Asian Ceramic Societies, 8(1), 1–9. ods for preparation of Elrahman, N. K. (2024). Physical meth-Harbi, N., & Abd-Al Qura -nanomaterials their characterization and applications: A review. Journal of Umm Al 7-00165-024-https://doi.org/10.1007/s43994 .377–University for Applied Sciences, 1

2